Sains Malaysiana 53(6)(2024): 1441-1461
http://doi.org/10.17576/jsm-2024-5306-17

A Robust Design for the Omnibus SPRT Control Chart Under Skewed Data Distributions

(Reka Bentuk Teguh untuk Carta Kawalan Omnibus SPRT di Bawah Taburan Data Pencong)

Jing Wei Teoh[1], Wei Lin Teoh[1,2,*], Zhi Lin Chong[3], Ming Ha Lee[4] & Khai Wah Khaw[5]

[1]*School of Mathematical and Computer Sciences, Heriot-Watt University Malaysia, 62200 Putrajaya, Malaysia*
[2]*International Chair in DS & XAI, International Research Institute for Artificial Intelligence and Data Science, Dong A University, Danang, Vietnam*
[3]*Department of Electronic Engineering, Faculty of Engineering and Green Technology, Universiti Tunku Abdul Rahman, 31900 Kampar, Perak, Malaysia*
[4]*Faculty of Engineering, Computing and Science, Swinburne University of Technology Sarawak Campus, 93350 Kuching, Sarawak, Malaysia*
[5]*School of Management, Universiti Sains Malaysia, 11800 Gelugor, Pulau Pinang, Malaysia*

Received: 18 December 2023/Accepted: 23 May 2024

ABSTRACT

Control charts are widely used in manufacturing industries to ensure that production levels are stable and satisfactory. Recently, the omnibus sequential probability ratio test (OSPRT) control chart was developed for the purpose of monitoring the mean and variability of a process simultaneously. As the OSPRT chart was proposed for the first time in literature, its development relied entirely on the assumption that data follow the Normal distribution. Nonetheless, researchers are frequently reminded that the quality characteristics of manufacturing processes do not necessarily follow the Normal distribution, e.g., strengths of glass fibres, and lifetimes of products. In this paper, we investigate the extent to which the performances of the OSPRT chart designed for the Normal model deteriorate, in situations where the data distributions are Gamma and Lognormal. Results show that the in-control average run length (ARL) and standard deviation of the run length of the OSPRT chart designed for the Normal distribution deteriorate rapidly as skewness increases. To address this issue, we propose a robust design for the OSPRT chart by adjusting its control limits, known as the skewness correction method. It is shown that the skewness-corrected OSPRT chart enjoys a guaranteed in-control ARL, with a justifiable degradation in its out-of-control performances. Besides, we also show some insights into selecting the charting parameters for the skewness-corrected OSPRT chart in order to achieve an optimum out-of-control ARL performance over various shift sizes. The paper wraps up with an illustrative example of the skewness-corrected OSPRT chart for monitoring the weights of radial tyres.

Keywords: Average run length; joint monitoring control chart; sequential probability ratio test; skewed distributions; statistical process control

ABSTRAK

Carta kawalan telah digunakan secara meluas dalam sektor pembuatan untuk memastikan bahawa tahap pengeluaran adalah stabil dan memuaskan. Baru-baru ini, carta kawalan berdasarkan ujian nisbah kebarangkalian berjujukan (OSPRT) telah direka untuk tujuan memantau min dan variabiliti sesuatu proses industri secara serentak. Oleh sebab carta OSPRT baharu diusulkan, rekaannya bergantung sepenuhnya pada andaian bahawa data mengikuti taburan Normal. Walau bagaimanapun, para penyelidik sering diingatkan bahawa ciri mutu dalam proses pembuatan tidak semestinya mengikuti taburan Normal, seperti kekuatan serat kaca dan hayat produk. Dalam makalah ini, kami mengkaji sejauh mana prestasi carta OSPRT yang direka untuk taburan Normal merosot, dalam situasi yang mana taburan data adalah Gamma dan Lognormal. Hasil kajian menunjukkan bahawa purata panjang larian (ARL) dan sisihan piawai panjang larian carta OSPRT bagi kes terkawal merosot dengan laju apabila darjah pencongan meningkat. Untuk menyelesaikan masalah ini, kami membina reka bentuk yang teguh untuk carta OSPRT dengan mengubahsuaikan had kawalan, dikenali sebagai kaedah pembetulan pencongan. Carta OSPRT berdasarkan pembetulan pencongan didapati menghasilkan ARL terkawal yang terjamin, dan prestasinya dalam kes tidak terkawal juga kurang dijejaskan. Selain itu, kami memberikan beberapa garis panduan untuk memilih parameter carta OSPRT yang sesuai bagi mencapai prestasi ARL tidak terkawal yang optimum untuk pelbagai magnitud anjakan. Makalah ini diakhiri dengan contoh aplikasi carta OSPRT berdasarkan pembetulan pencongan untuk memantau berat tayar radial.

Kata kunci: Carta kawalan pemantauan serentak; kawalan proses statistik; purata panjang larian; taburan pencong; ujian nisbah kebarangkalian berjujukan

Introduction

Statistical process control (SPC), which constitutes a decent part of applied statistics, is widely recognised as the most effective technique for monitoring a process quality characteristic of interest. Among a myriad of tools available, the control chart distinguishes itself as the most popular SPC tool, thanks to its simplicity and visually intuitive representation. In order to address the rising demand for control charts with greater sensitivity, various researchers have contributed to ongoing enhancements of the state-of-the-art techniques (Abu-Shawiesh &Abdullah 2001; Khoo 2004; Li et al. 2010; Teh et al. 2015). Typical developments include the modification of existing control schemes or designs to achieve certain aims (Abu-Shawiesh & Abdullah 2001; Teh et al. 2015), and the development of new control schemes based on insights from past research and/or unexplored knowledge areas (Khoo 2004; Li, Tang & Ng 2010). As control charts are fundamental tools in industrial statistics, they often prove useful in a diverse range of applications spanning various industries, such as biotechnology, manufacturing, signal processing, and finance, to name a few.

The main goal of SPC was to improve the quality of processes by identifying and reducing variation and errors, ultimately leading to higher consistency in the final output. Having that said, it is essential for practitioners to control both the location and variability of a process in any quality control application. There is a considerable number of joint monitoring control charts devised for this purpose, each possessing a different feature catered to specific scenarios in the real industrial environment. For instance, Haq, Brown and Moltchanova (2015) and Sabahno, Amiri and Castagliola (2021) devised joint monitoring control charts for the mean and variance based on the assumption that the process follows a Normal (or Gaussian) distribution. Considering that certain manufacturing processes may exhibit non-Normal or skewed distributions, researchers such as Chowdhury, Mukherjee and Chakraborti (2015), Diaz Pulido, Cordero Franco and Tercero Gómez (2023) and Hou and Yu (2021), have developed nonparametric control charts that are sensitive to changes in both the location and scale parameters of a distribution. Recently, Teoh et al. (2023) proposed a new sequential probability ratio test (SPRT) chart, known as the omnibus SPRT (OSPRT) chart, for simultaneous monitoring of the mean and variance of a Normal distribution. They showed that the OSPRT chart not only outperforms the Shewhart $\underline{X}$-S, weighted-loss cumulative sum (CUSUM), and absolute-value SPRT charts in terms of the detection speed, but also enjoys global optimal properties with respect to the out-of-control average time to signal. In addition to the outstanding detection performance, the OSPRT chart is also shown to yield a relatively small in-control average sample number in the long run, making it extremely appealing to production applications where sampling is expensive.

As stated in the preceding paragraph, the OSPRT chart operates on the assumption that the underlying data follow the Normal distribution. However, in certain applications, the shape of the data can differ substantially from that of the Normal distribution. Some examples of data include the strength of glass fibres, economic indices, lifetimes of products, and air pollution levels. The distributions of these data are typically skewed to the right (Dakhn, Bakar & Ibrahim 2023; Farouk, Aziz & Zain 2020; Hossain et al. 2022; Nawaz, Azam & Aslam 2021; Qiu 2018). Generally, control charts designed for the Normal distribution are expected to perform less satisfactorily under non-Normal conditions. This is made worse when the underlying data have a highly skewed distribution. Many researchers have reported deterioration in the performance of control charts designed under the Normal model when the data in use follow a skewed distribution (Ho, Kao & Chou 2021; Huberts et al. 2018; Noorossana, Fathizadan & Nayebpour 2016). There are three common ways to tackle this issue. First, if practitioners know the exact distribution of the data, then it would be possible to derive a parametric control chart for the specific distribution. One example is the SPRT chart for the Maxwell distribution proposed by Godase, Mahadik and Rakitzis (2022). One of the challenges of such a method is that the statistic of the control chart can be extremely convoluted and may not have a very neat form. It may also be difficult to derive the run length properties of the control chart due to the perplexity in its control statistic. The second approach is to derive a nonparametric control chart which is well-suited for a range of distributions. One example is the SPRT sign chart proposed by Mahadik and Godase (2023). While the approach is quite popular among scholars, we quickly realise that nonparametric control charts tend to have a lower statistical power compared to parametric control charts, especially in settings where parametric assumptions are approximately valid. The third approach, which is adopted in this paper, is to introduce skewness correction to control charts designed under the Normal model (Huberts et al. 2018; Mehmood et al. 2020; Riaz et al. 2016). This is done by modifying the control limits of the control chart to achieve the desired in-control average run length (ARL), while preserving the original features of the control chart. The biggest advantage of this approach is that we avoid revamping the entire control chart, which can often be quite tedious and cumbersome. By preserving the structure of the original control chart, practitioners will find the design and operation of the skewness-corrected control chart simpler and less demanding. In this research, we investigate the performances of the OSPRT chart under two different skewed distributions, and develop a new robust design for the OSPRT chart based on skewness correction. The proposed design guarantees that the in-control performance of the OSPRT chart is kept at the desired level, with the price of a degraded out-of-control performance that depends upon the degree of skewness. This paper also aims to provide some insights into selecting appropriate charting parameters for the OSPRT chart in order to maximise its effectiveness towards a range of process shifts. It is, however, important to note that any attempt to compare the OSPRT chart with other control charts is far beyond the scope of this paper, and hence is not discussed throughout the paper.

The paper is organised as follows. We first provide an overview of the OSPRT chart designed under the Normal model. This includes a step-by-step implementation of the OSPRT chart, as well as its run length profiles when the underlying data are Normally distributed. Next, we present the statistical properties of two popular choices of skewed distributions, i.e., the Gamma and Lognormal distributions. We then evaluate the ARL and standard deviation of the run length (SDRL) performances of the conventional OSPRT chart under the Gamma and Lognormal distributions for various degrees of skewness. The results obtained are contrasted against the performances obtained under the Normal distribution. Next, we outline the full procedure for computing the skewness-corrected control limits for the OSPRT chart, and present some analyses on the possible regions where the optimal charting parameters lie. An illustrative example on the implementation of the OSPRT chart with skewness correction is also presented. Finally, some conclusions and suggestions for future work are provided.

THE OSPRT CHART FOR THE NORMAL DISTRIBUTION

Let X denote the quality characteristic of a Normal process with mean μ_0 and variance σ_0^2. During process monitoring, the realisations of the process (X_{i1}, X_{i2}, …, X_{iN_i} are sampled sequentially at the sampling points i = 1, 2, …, where N_i indicates the sample number of the ith sample index. It is assumed that the observations are sampled independently from the process. Suppose that our goal is to detect a change in the distribution from $N(\mu_0,\sigma_0^2)$ to $N(\mu_0 + \delta\sigma_0, \eta^2\, \sigma_0^2)$, where δ and η represent the magnitudes of the mean and standard deviation shifts, respectively. The OSPRT chart for monitoring the sequence of observations has the following control statistic

$$C_{i,j} = C_{i,j-1} + sgn(\eta - 1)\left(\frac{X_{i,j} - \mu_0}{\sigma_0} + k\right)^2 - \gamma, \quad C_{i,0} = 0, \tag{1}$$

for i = 1, 2, … and j = 1, 2, …, N_i, where $sgn(\cdot)$ is the sign function, and (k, γ) are the reference parameters of the OSPRT chart. Teoh et al. (2023) proved that the out-of-control ARL (ARL_1) for a pair of deterministic shift sizes (δ, η) can be minimised by choosing

$$k = \frac{\delta}{\eta^2 - 1} \tag{2}$$

and

$$\gamma = \frac{\delta^2\eta^2}{(\eta^2-1)^2} + \frac{2\eta^2 \ln \eta}{\eta^2-1}. \tag{3}$$

It is worth noting that $\gamma > 0$ for all values of δ and η, whereas the sign of k depends on the directions of the mean shift and/or standard deviation shift. Throughout this paper, we will consider only the case $\delta > 0$ and $\eta > 1$, as the operation of the lower-sided OSPRT chart is identical to its upper-sided counterpart. The control statistic of the upper-sided OSPRT chart is reduced to the following:

$$C_{i,j} = C_{i,j-1} + \left(\frac{X_{i,j} - \mu_0}{\sigma_0} + k\right)^2 - \gamma, \qquad C_{i,0} = 0, \quad (4)$$

since $sgn(\cdot) = 1$ when $\eta > 1$.

The OSPRT chart operates on two control limits, i.e., a lower control limit g (also known as the acceptance limit) and an upper control limit h (also known as the rejection limit). Immediately after an observation is sampled, a decision on the status of the process is reviewed according to the position of the control statistic on the charting region. In particular, after the jth measurement is taken in the ith OSPRT, a) if $C_{i,j}$ drops in the region below g, the process is said to be in-control, b) if $C_{i,j}$ falls in the region above h, the process is said to be out-of-control, and c) if $C_{i,j}$ falls in the region between g and h, the status of the process is indeterminate, and another measurement is sought.

Generally, when the process is declared as in-control, sampling will be terminated and the practitioner will resume sampling after a designated period of time. When the process is flagged as out-of-control, the affected production line is immediately suspended, and the relevant engineer attends to investigate the root cause(s) of the issue and eliminate them as soon as possible.

To assess the run-length performances of the OSPRT chart, we provide the formulae for the average sample number (ASN), ARL, and SDRL metrics as functions of (δ, η). Since each SPRT samples a random number of observations, the ASN serves an important role in measuring the expected number of samples required until a decision about the process can be reached. To derive the aforementioned properties, we adopt the Markov chain method with two absorbing states. The proof begins by partitioning the interval $[g, h]$ into a large number of subintervals, say M. The sequence of subintervals $[g, g + \Delta]$, $[g + \Delta, g + 2\Delta]$, ……, $[g + (M - 1)\Delta, h]$ are taken as the transient states $S_1, S_2, ……, S_M$ of the Markov chain, respectively, where $\Delta = (h - g)/M$ is the length of each subinterval. Besides, we denote $(-\infty, g)$ and (h, ∞) as the acceptance state S_g and the rejection state S_h, respectively. The transition probability matrix $\mathbf{P}$ can be constructed as follows:

$$\mathbf{P} = \begin{pmatrix} p_{1,1} & p_{1,2} & \cdots & p_{1,M} \\ p_{2,1} & p_{2,2} & \cdots & p_{2,M} \\ \vdots & \vdots & \ddots & \vdots \\ p_{M,1} & p_{M,2} & \cdots & p_{M,M} \end{pmatrix}, \quad (5)$$

where $p_{u,v}$ is the probability of transiting from state S_u to state S_v in a single step, for $u, v = 1, 2, …, M$, with the expression

$$p_{u,v} = \chi_1^2\left[\frac{\Delta(v-u+0.5)+\gamma}{\eta^2} \,\middle|\, \left(\frac{\delta+k}{\eta}\right)^2\right] - \chi_1^2\left[\frac{\Delta(v-u-0.5)+\gamma}{\eta^2} \,\middle|\, \left(\frac{\delta+k}{\eta}\right)^2\right]. \quad (6)$$

Here, $\chi_1^2\{\cdot \mid [(\delta + k)/\eta]^2\}$ is the cumulative distribution function (CDF) of the non-central chi-squared distribution with one degree of freedom and non-centrality parameter $[(\delta + k) / \eta]^2$.

In the following step, we construct a row vector $\mathbf{B} = (b_1, b_2, …, b_M)$, where b_u is the probability that the control statistic jumps from the initial state to state S_u. The expression for b_u is given by

$$b_u = \chi_1^2\left[\frac{g+\Delta\cdot u+\gamma}{\eta^2} \,\middle|\, \left(\frac{\delta+k}{\eta}\right)^2\right] - \chi_1^2\left[\frac{g+\Delta\cdot(u-1)+\gamma}{\eta^2} \,\middle|\, \left(\frac{\delta+k}{\eta}\right)^2\right], \quad (7)$$

for $u = 1, …, M$. The ASN is then calculated using the following matrix-vector equation

$$ASN = 1 + \mathbf{B}(\mathbf{I} - \mathbf{P})^{-1}\mathbf{1}, \quad (8)$$

where $\mathbf{1}$ is a $M \times 1$ vector with entries equal to one, and $\mathbf{I}$ is the $M \times M$ identity matrix.

The ARL and SDRL are comprehensive metrics used to evaluate the expected value and the variability of the run length distribution, respectively. To calculate the aforementioned metrics, it is required to first compute the probability that a single OSPRT accepts the process as in-control, conditional on the shift sizes (δ, η). This probability $OC(\delta, \eta)$ can be expressed via the following matrix-vector equation

$$OC(\delta, \eta) = q_0 + \mathbf{B}(\mathbf{I} - \mathbf{P})^{-1}\mathbf{R}. \quad (9)$$

Here, the quantity q_0 represents the probability that the control statistic jumps from the initial state to the acceptance state S_g in a single step, whereas $\mathbf{B}(\mathbf{I} - \mathbf{P})^{-1}\mathbf{R}$ represents the probability that the control statistic transits from the initial state to the acceptance state in more than one step. The expression for q_0 is given by

$$q_0 = \chi_1^2\left[\frac{g+\gamma}{\eta^2} \mid \left(\frac{\delta+k}{\eta}\right)^2\right]. \tag{10}$$

R is a column vector $(r_1, r_1, \ldots, r_M)^{\mathsf{T}}$, where r_u is the probability that the control statistic jumps from state S_u to the acceptance state S_g in a single step. The expression for r_u is given by

$$r_u = \chi_1^2\left[\frac{\Delta\cdot(0.5-u)+\gamma}{\eta^2} \mid \left(\frac{\delta+k}{\eta}\right)^2\right]. \tag{11}$$

As the run length (RL) is defined as the number of samples required until a signal is produced, it is well-known that RL follows the geometric distribution with probability $1 - \mathrm{OC}(\delta,\eta)$ (Montgomery 2019; Stoumbos & Reynolds Jr. 1997). By using the properties of a geometric distribution, the ARL and SDRL of the OSPRT chart can be derived as

$$ARL = \frac{1}{1-OC(\delta,\eta)} \tag{12}$$

and

$$SDRL = \sqrt{\frac{OC(\delta,\eta)}{[1-OC(\delta,\eta)]^2}}, \tag{13}$$

respectively.

THE GAMMA AND LOGNORMAL DISTRIBUTIONS

This section discusses some of the statistical properties of the Gamma and Lognormal distributions, i.e., the in-control mean (μ_0^*), in-control standard deviation (σ_0^*), and Pearson's moment coefficient of skewness (θ). Both distributions are chosen in our study as they accurately describe the behaviour of many skewed variables, such as product lifetimes, times to failure of devices, and air pollution indices (Abd Razak, Zubairi & Yunus 2014; Dakhn, Bakar & Ibrahim 2023; Farouk, Aziz & Zain 2020). Besides, the degree of skewness of these distributions can be easily adjusted by tuning either the shape or scale parameter.

The probability density function (pdf) of the Gamma distribution is $f_Z(z) = \beta^\alpha z^{\alpha-1} e^{-\beta z}/\Gamma(\alpha)$, where $\alpha > 0$ and $\beta > 0$ are the shape and rate parameters of the Gamma distribution, respectively, and $\Gamma(\cdot)$ is the gamma function. The CDF of the Gamma distribution does not have a specific closed form. It is simply expressed as $F_Z(z) = \int_0^z f_Z(z)\, dz$ (with some abuse of notation), and can be evaluated via numerical integration. It is known that the skewness of the Gamma distribution depends only on the shape parameter α. Hence, we set $\beta = 1$ throughout this paper for ease of computation. The formulae for the mean, standard deviation, and coefficient of skewness of the Gamma distribution are (Zwillinger & Kokoska 1999)

$$\mu_0^* = \alpha, \tag{14}$$

$$\sigma_0^* = \sqrt{\alpha}, \tag{15}$$

and

$$\theta = \frac{2}{\sqrt{\alpha}}, \tag{16}$$

respectively.

The pdf of the Lognormal distribution is $f_Z(z) = exp\,[-(ln\, z - \mu_{LN})^2/(2\sigma_{LN}^{\ 2})]/(z\sigma_{LN}\sqrt{2\pi})$, where μ_{LN} and $\sigma_{LN} > 0$ are the location and scale parameters of the Lognormal distribution, respectively. The CDF of the Lognormal distribution can be shown as $F_Z(z) = \Phi\,[(ln\, z - \mu_{LN})/\sigma_{LN}]$. Since the skewness of the Lognormal distribution is independent of the location parameter, we set $\mu_{LN} = 0$ for the sake of simplicity. The formulae for the mean, standard deviation, and coefficient of skewness of the Lognormal distribution are (Zwillinger & Kokoska 1999)

$$\mu_0^* = exp\left(\frac{\sigma_{LN}^2}{2}\right), \tag{17}$$

$$\sigma_0^* = \sqrt{exp\,(2\sigma_{LN}^2) - exp\,(\sigma_{LN}^2)}, \tag{18}$$

and

$$\theta = \left[exp\,(\sigma_{LN}^2) + 2\right]\sqrt{exp\,(\sigma_{LN}^2) - 1}, \tag{19}$$

respectively.

THE IMPACT OF SKEWNESS ON THE PERFORMANCES OF THE OSPRT CHART DESIGNED UNDER THE NORMAL MODEL

In this section, we analyse the performances of the OSPRT chart designed for the Normal distribution in cases where non-normal data are used. Prior to the investigation, it is necessary to specify the relevant parameters for designing the OSPRT chart. In this study, we consider a false alarm rate of 0.27%, which is equivalent to an in-control ARL (ARL_0) of $\tau = 370.4$, and an in-control

ASN (ASN_0) equal to five. It should be noted that there is an infinite number of possible combinations (k, γ) by which the OSPRT chart can be constructed. To provide a well-rounded exploratory analysis, we consider six different combinations of (k, γ) from a multitude of sizes, i.e., $(k, \gamma) \in \{(0.1, 1.5), (0.1, 4.0), (0.5, 2.0), (0.5, 5.0), (1.0, 2.5), (1.0, 6.0)\}$. The control limits (g, h) can then be determined via some root-finding algorithms (e.g., the Newton-Raphson algorithm) to meet the specifications on the ARL_0 and ASN_0.

Table 1 tabulates the control limits (g, h) of the OSPRT chart designed under the Normal model for the six pairs of (k, γ), together with the (ARL, SDRL) values for $\delta \in \{0.0, 0.5, 1.0, 1.5, 2.0\}$ and $\eta \in \{1.0, 1.5, 2.0\}$. The performance metrics are computed using Equations (12) and (13), and all the results have been verified with Monte Carlo simulation. As a numeric example, when the reference parameters $(k, \gamma) = (0.5, 2.0)$ are chosen, the control limits are calculated as $g = -3.060$ and $h = 16.896$, and the resulting out-of-control ARL (ARL_1) and out-of-control SDRL ($SDRL_1$) values at $(\delta, \eta) = (0.5, 1.5)$ are equal to 1.66 and 1.05, respectively. From Table 1, it is observed that different combinations of (k, γ) result in varying performances over different shift sizes (δ, η). For instance, the reference parameters $(k, \gamma) = (0.1, 1.5)$ is the best combination for the case when only the variance shift occurs, i.e., $\delta = 0.0$ and $\eta > 1.0$. In particular, the associated (ARL_1, $SDRL_1$) values are equal to (2.11, 1.53) and (1.31, 0.64) at $\eta = 1.5$ and $\eta = 2.0$, respectively. When the expected shift sizes are $(\delta, \eta) = (0.5, 1.5)$, the combination $(k, \gamma) = (0.5, 2.0)$ is preferred as it produces the lowest (ARL_1, $SDRL_1$) among the six combinations, i.e., (ARL_1, $SDRL_1$) = (1.66, 1.05). This observation is consistent with the optimality property of the OSPRT chart, which states that the combination (k, γ) tuned in Equations (2) and (3) is optimal with respect to the ARL_1 for any deterministic shift sizes (δ, η).

TABLE 1. Control limits (g, h) and the corresponding (ARL, SDRL) values of the OSPRT chart designed under the Normal model, for $ARL_0 = \tau = 370.4$, $ASN_0 = 5$, and $(k, \gamma) \in \{(0.1, 1.5), (0.1, 4.0), (0.5, 2.0), (0.5, 5.0), (1.0, 2.5), (1.0, 6.0)\}$, when the underlying distribution is Normal

(k, γ)		(0.1, 1.5)	(0.1, 4.0)	(0.5, 2.0)	(0.5, 5.0)	(1.0, 2.5)	(1.0, 6.0)
(g, h)		(–1.876, 15.863)	(–13.365, 5.875)	(–3.060, 16.896)	(–16.779, 6.628)	(–1.773, 33.345)	(–17.499, 9.806)
δ	η	(ARL, SDRL)	(ARL, SDRL)	(ARL, SDRL)	(ARL, SDRL)	(ARL, SDRL)	(ARL, SDRL)
0.0	1.0	(370.40, 369.90)	(370.40, 369.90)	(370.40, 369.90)	(370.40, 369.90)	(370.40, 369.90)	(370.40, 369.90)
	1.5	(2.11, 1.53)	(8.03, 7.52)	(2.75, 2.19)	(11.38, 10.87)	(4.01, 3.48)	(12.26, 11.75)
	2.0	(1.31, 0.64)	(1.84, 1.24)	(1.38, 0.73)	(2.40, 1.83)	(2.08, 1.50)	(2.86, 2.30)
0.5	1.0	(17.61, 17.10)	(92.38, 91.88)	(6.14, 5.62)	(59.83, 59.33)	(2.67, 2.11)	(41.44, 40.93)
	1.5	(1.74, 1.13)	(5.02, 4.49)	(1.66, 1.05)	(4.90, 4.37)	(2.02, 1.44)	(4.07, 3.54)
	2.0	(1.27, 0.59)	(1.63, 1.01)	(1.27, 0.58)	(1.79, 1.18)	(1.70, 1.09)	(1.81, 1.21)
1.0	1.0	(1.80, 1.20)	(14.55, 14.04)	(1.30, 0.62)	(8.74, 8.22)	(1.30, 0.62)	(4.08, 3.54)
	1.5	(1.36, 0.70)	(2.37, 1.81)	(1.24, 0.54)	(2.08, 1.50)	(1.45, 0.80)	(1.67, 1.05)
	2.0	(1.19, 0.48)	(1.33, 0.66)	(1.16, 0.43)	(1.34, 0.67)	(1.44, 0.80)	(1.30, 0.62)
1.5	1.0	(1.13, 0.38)	(2.32, 1.75)	(1.04, 0.20)	(1.55, 0.93)	(1.08, 0.29)	(1.10, 0.33)
	1.5	(1.15, 0.42)	(1.33, 0.66)	(1.08, 0.30)	(1.21, 0.51)	(1.21, 0.50)	(1.11, 0.34)
	2.0	(1.12, 0.37)	(1.13, 0.39)	(1.09, 0.31)	(1.11, 0.36)	(1.28, 0.60)	(1.09, 0.31)
2.0	1.0	(1.02, 0.14)	(1.05, 0.22)	(1.00, 0.06)	(1.01, 0.10)	(1.02, 0.14)	(1.00, 0.03)
	1.5	(1.06, 0.25)	(1.05, 0.24)	(1.03, 0.16)	(1.03, 0.17)	(1.10, 0.33)	(1.01, 0.11)
	2.0	(1.07, 0.27)	(1.04, 0.21)	(1.04, 0.21)	(1.03, 0.18)	(1.17, 0.45)	(1.02, 0.15)

To evaluate the performances of the Normal-designed OSPRT chart under skewed distributions, we first select a set of skewness levels θ to be considered in our study. In this paper, we present results for $\theta \in \{1.0, 2.0, 3.0\}$ using both the Gamma and Lognormal distributions. Note that the shape or scale parameters of the Gamma and Lognormal distributions can be tuned to achieve a specific degree of skewness. For example, to achieve a skewness of $\theta = 2.0$, the shape parameter α of the Gamma distribution must satisfy the equation $2/\sqrt{\alpha}$ = 2.0 (from Equation (16)), giving $\alpha = 1$; whereas the scale parameter σ_{LN}^2 of the Lognormal distribution must satisfy the equation $[exp\ (\sigma_{LN}^2) + 2]\sqrt{exp\ (\sigma_{LN}^2) - 1}$ = 2.0 (from Equation (19)), giving $\sigma_{LN} = 0.5514$ with the aid of some root-finding algorithms. Tables 2 and 3 show the (ARL, SDRL) values of the Normal-designed OSPRT chart in cases where the underlying distributions of data are Gamma and Lognormal, respectively, for $\theta \in \{1.0, 2.0, 3.0\}$. As a numeric example, when $\theta = 2.0$ and $\alpha = 1.0000$ for the Gamma distribution, the (ARL_1, $SDRL_1$) values of the OSPRT chart with reference parameters $(k, \gamma) = (1.0, 2.5)$ are equal to (1.84, 1.24) at $(\delta, \eta) = (1.0, 1.5)$. It is worth noting that, since the data do not follow the usual Normal distribution, the run-length properties of the OSPRT chart cannot be evaluated using the formulae detailed in Equations (6), (7), (10), and (11). Therefore, in Tables 2 and 3, we have produced all the results through Monte Carlo simulation with 100,000 replications.

TABLE 2. The (ARL, SDRL) values of the OSPRT chart designed under the Normal model, for $ARL_0 = \tau = 370.4$, $ASN_0 = 5$, and $(k, \gamma) \in \{(0.1, 1.5), (0.1, 4.0), (0.5, 2.0), (0.5, 5.0), (1.0, 2.5), (1.0, 6.0)\}$, when the underlying distribution is Gamma with skewness $\theta \in \{1.0, 2.0, 3.0\}$

			(k, γ)	(0.1, 1.5)	(0.1, 4.0)	(0.5, 2.0)	(0.5, 5.0)	(1.0, 2.5)	(1.0, 6.0)
			(g, h)	(–1.876, 15.863)	(–13.365, 5.875)	(–3.060, 16.896)	(–16.779, 6.628)	(–1.773, 33.345)	(–17.499, 9.806)
α	θ	δ	η	(ARL, SDRL)	(ARL, SDRL)	(ARL, SDRL)	(ARL, SDRL)	(ARL, SDRL)	(ARL, SDRL)
4.0000	1.0	0.0	1.0	(61.95, 61.44)	(47.14, 46.64)	(46.22, 45.72)	(41.15, 40.64)	(76.92, 76.42)	(39.98, 39.48)
			1.5	(2.64, 2.08)	(6.74, 6.22)	(4.10, 3.56)	(7.01, 6.49)	(6.73, 6.21)	(7.01, 6.49)
			2.0	(1.36, 0.70)	(2.25, 1.67)	(1.67, 1.06)	(2.83, 2.28)	(3.10, 2.55)	(3.13, 2.59)
		0.5	1.0	(13.80, 13.29)	(19.96, 19.46)	(6.80, 6.28)	(16.15, 15.65)	(3.66, 3.12)	(13.26, 12.75)
			1.5	(2.51, 1.95)	(4.35, 3.82)	(2.44, 1.87)	(4.06, 3.53)	(2.89, 2.34)	(3.66, 3.12)
			2.0	(1.45, 0.81)	(2.05, 1.47)	(1.59, 0.97)	(2.17, 1.60)	(2.38, 1.81)	(2.18, 1.60)
		1.0	1.0	(2.49, 1.93)	(7.34, 6.83)	(1.51, 0.88)	(5.46, 4.93)	(1.33, 0.66)	(3.49, 2.95)
			1.5	(1.80, 1.20)	(2.59, 2.03)	(1.52, 0.89)	(2.28, 1.71)	(1.68, 1.07)	(1.91, 1.32)
			2.0	(1.42, 0.77)	(1.67, 1.05)	(1.39, 0.74)	(1.63, 1.02)	(1.81, 1.21)	(1.55, 0.93)
		1.5	1.0	(1.19, 0.47)	(2.37, 1.80)	(1.03, 0.18)	(1.69, 1.08)	(1.02, 0.15)	(1.15, 0.42)
			1.5	(1.32, 0.65)	(1.57, 0.95)	(1.15, 0.41)	(1.38, 0.72)	(1.22, 0.52)	(1.19, 0.48)
			2.0	(1.29, 0.61)	(1.34, 0.67)	(1.21, 0.50)	(1.27, 0.59)	(1.43, 0.78)	(1.20, 0.49)
		2.0	1.0	(1.01, 0.09)	(1.08, 0.30)	(1.00, 0.01)	(1.01, 0.12)	(1.00, 0.00)	(1.00, 0.02)
			1.5	(1.09, 0.32)	(1.12, 0.37)	(1.02, 0.16)	(1.06, 0.24)	(1.05, 0.22)	(1.02, 0.13)
			2.0	(1.15, 0.42)	(1.13, 0.38)	(1.08, 0.30)	(1.08, 0.30)	(1.19, 0.48)	(1.05, 0.23)
1.0000	2.0	0.0	1.0	(34.62, 34.12)	(22.37, 21.87)	(27.09, 26.58)	(20.62, 20.11)	(48.79, 48.28)	(20.39, 19.88)
			1.5	(4.60, 4.07)	(6.01, 5.49)	(6.03, 5.51)	(6.14, 5.62)	(10.16, 9.64)	(6.27, 5.75)
			2.0	(1.63, 1.02)	(2.90, 2.35)	(2.71, 2.15)	(3.27, 2.73)	(5.44, 4.92)	(3.51, 2.97)
		0.5	1.0	(13.51, 13.00)	(12.52, 12.01)	(7.76, 7.24)	(10.79, 10.27)	(4.89, 4.36)	(9.43, 8.91)
			1.5	(4.22, 3.69)	(4.41, 3.87)	(3.58, 3.03)	(4.11, 3.57)	(4.01, 3.48)	(3.83, 3.29)
			2.0	(2.21, 1.64)	(2.59, 2.03)	(2.48, 1.91)	(2.61, 2.05)	(3.58, 3.04)	(2.60, 2.04)

continue to next page

continue from previous page

		1.0	1.0	(3.36, 2.81)	(6.18, 5.65)	(1.73, 1.12)	(4.89, 4.36)	(1.25, 0.56)	(3.51, 2.97)
			1.5	(2.53, 1.97)	(2.93, 2.37)	(1.89, 1.29)	(2.58, 2.02)	(1.84, 1.24)	(2.20, 1.62)
			2.0	(2.11, 1.53)	(2.09, 1.51)	(1.86, 1.26)	(1.97, 1.39)	(2.22, 1.64)	(1.85, 1.25)
		1.5	1.0	(1.19, 0.48)	(2.57, 2.00)	(1.01, 0.07)	(1.87, 1.27)	(1.00, 0.00)	(1.21, 0.50)
			1.5	(1.50, 0.86)	(1.84, 1.24)	(1.16, 0.43)	(1.57, 0.94)	(1.09, 0.31)	(1.29, 0.61)
			2.0	(1.61, 0.99)	(1.61, 0.99)	(1.35, 0.69)	(1.47, 0.83)	(1.44, 0.79)	(1.33, 0.66)
		2.0	1.0	(1.00, 0.00)	(1.12, 0.36)	(1.00, 0.00)	(1.01, 0.11)	(1.00, 0.00)	(1.00, 0.00)
			1.5	(1.06, 0.24)	(1.20, 0.49)	(1.00, 0.03)	(1.08, 0.29)	(1.00, 0.00)	(1.01, 0.10)
			2.0	(1.23, 0.53)	(1.24, 0.55)	(1.06, 0.26)	(1.14, 0.41)	(1.04, 0.22)	(1.06, 0.26)
0.4444	3.0	0.0	1.0	(28.75, 28.25)	(16.84, 16.34)	(23.28, 22.77)	(15.86, 15.35)	(44.23, 43.73)	(15.81, 15.30)
			1.5	(7.42, 6.90)	(6.23, 5.71)	(7.92, 7.41)	(6.20, 5.67)	(13.50, 12.99)	(6.44, 5.92)
			2.0	(2.88, 2.32)	(3.52, 2.98)	(4.39, 3.85)	(3.83, 3.29)	(8.23, 7.72)	(4.13, 3.59)
		0.5	1.0	(14.38, 13.87)	(10.78, 10.26)	(9.00, 8.48)	(9.54, 9.02)	(5.90, 5.38)	(8.60, 8.08)
			1.5	(5.86, 5.34)	(4.77, 4.24)	(4.74, 4.21)	(4.45, 3.92)	(5.37, 4.84)	(4.19, 3.65)
			2.0	(3.82, 3.28)	(3.16, 2.61)	(3.54, 3.00)	(3.07, 2.53)	(4.87, 4.34)	(3.06, 2.51)
		1.0	1.0	(4.35, 3.82)	(6.12, 5.59)	(1.91, 1.32)	(4.95, 4.42)	(1.12, 0.36)	(3.74, 3.20)
			1.5	(3.36, 2.82)	(3.35, 2.81)	(2.25, 1.67)	(2.95, 2.39)	(1.73, 1.13)	(2.52, 1.96)
			2.0	(2.89, 2.33)	(2.52, 1.96)	(2.33, 1.76)	(2.34, 1.77)	(2.52, 1.95)	(2.16, 1.58)
		1.5	1.0	(1.11, 0.34)	(2.84, 2.29)	(1.00, 0.00)	(2.07, 1.49)	(1.00, 0.00)	(1.25, 0.56)
			1.5	(1.60, 0.98)	(2.13, 1.55)	(1.09, 0.31)	(1.77, 1.16)	(1.00, 0.00)	(1.37, 0.72)
			2.0	(1.90, 1.31)	(1.90, 1.30)	(1.36, 0.69)	(1.68, 1.07)	(1.21, 0.51)	(1.45, 0.81)
		2.0	1.0	(1.00, 0.00)	(1.14, 0.40)	(1.00, 0.00)	(1.01, 0.08)	(1.00, 0.00)	(1.00, 0.00)
			1.5	(1.00, 0.01)	(1.27, 0.58)	(1.00, 0.00)	(1.09, 0.31)	(1.00, 0.00)	(1.00, 0.05)
			2.0	(1.13, 0.39)	(1.35, 0.68)	(1.00, 0.04)	(1.19, 0.47)	(1.00, 0.00)	(1.05, 0.23)

TABLE 3. The (ARL, SDRL) values of the OSPRT chart designed under the Normal model, for $ARL_0 = \tau = 370.4$, $ASN_0 = 5$, and $(k, \gamma) \in \{(0.1, 1.5), (0.1, 4.0), (0.5, 2.0), (0.5, 5.0), (1.0, 2.5), (1.0, 6.0)\}$, when the underlying distribution is Lognormal with skewness $\theta \in \{1.0, 2.0, 3.0\}$

			(k, γ)	(0.1, 1.5)	(0.1, 4.0)	(0.5, 2.0)	(0.5, 5.0)	(1.0, 2.5)	(1.0, 6.0)
			(g, h)	(–1.876, 15.863)	(–13.365, 5.875)	(–3.060, 16.896)	(–16.779, 6.628)	(–1.773, 33.345)	(–17.499, 9.806)
σ_{LN}	θ	δ	η	(ARL, SDRL)	(ARL, SDRL)	(ARL, SDRL)	(ARL, SDRL)	(ARL, SDRL)	(ARL, SDRL)
0.3143	1.0	0.0	1.0	(59.05, 58.54)	(44.64, 44.14)	(45.23, 44.73)	(39.54, 39.03)	(75.70, 75.20)	(38.58, 38.08)
			1.5	(2.72, 2.16)	(6.86, 6.34)	(4.16, 3.63)	(7.18, 6.67)	(6.75, 6.23)	(7.21, 6.69)
			2.0	(1.39, 0.73)	(2.26, 1.68)	(1.69, 1.08)	(2.87, 2.32)	(3.07, 2.52)	(3.20, 2.65)
		0.5	1.0	(14.11, 13.60)	(19.91, 19.40)	(6.92, 6.40)	(16.24, 15.73)	(3.62, 3.08)	(13.41, 12.90)
			1.5	(2.51, 1.95)	(4.46, 3.93)	(2.42, 1.85)	(4.17, 3.64)	(2.83, 2.28)	(3.75, 3.21)
			2.0	(1.46, 0.82)	(2.07, 1.49)	(1.58, 0.96)	(2.20, 1.62)	(2.32, 1.75)	(2.20, 1.63)
		1.0	1.0	(2.47, 1.90)	(7.52, 7.00)	(1.49, 0.86)	(5.59, 5.06)	(1.32, 0.65)	(3.56, 3.02)
			1.5	(1.77, 1.16)	(2.64, 2.08)	(1.49, 0.86)	(2.32, 1.74)	(1.65, 1.03)	(1.92, 1.33)
			2.0	(1.40, 0.75)	(1.67, 1.06)	(1.37, 0.71)	(1.63, 1.02)	(1.75, 1.15)	(1.55, 0.92)

continue to next page

continue from previous page

		1.5	1.0	(1.18, 0.46)	(2.40, 1.84)	(1.03, 0.18)	(1.70, 1.09)	(1.03, 0.17)	(1.15, 0.41)
			1.5	(1.29, 0.62)	(1.57, 0.95)	(1.14, 0.39)	(1.38, 0.72)	(1.21, 0.51)	(1.19, 0.47)
			2.0	(1.27, 0.58)	(1.33, 0.66)	(1.18, 0.47)	(1.26, 0.58)	(1.40, 0.74)	(1.19, 0.48)
		2.0	1.0	(1.01, 0.10)	(1.08, 0.30)	(1.00, 0.02)	(1.01, 0.12)	(1.00, 0.02)	(1.00, 0.02)
			1.5	(1.08, 0.30)	(1.12, 0.36)	(1.02, 0.16)	(1.05, 0.24)	(1.05, 0.24)	(1.01, 0.12)
			2.0	(1.14, 0.40)	(1.12, 0.36)	(1.07, 0.28)	(1.08, 0.29)	(1.19, 0.47)	(1.05, 0.22)
0.5514	2.0	0.0	1.0	(37.46, 36.96)	(24.31, 23.80)	(30.03, 29.53)	(22.54, 22.03)	(52.63, 52.13)	(22.31, 21.81)
			1.5	(4.48, 3.95)	(6.59, 6.07)	(6.06, 5.54)	(6.73, 6.21)	(10.05, 9.54)	(6.82, 6.30)
			2.0	(1.63, 1.01)	(2.97, 2.42)	(2.48, 1.92)	(3.41, 2.87)	(4.85, 4.32)	(3.68, 3.14)
		0.5	1.0	(14.78, 14.27)	(13.91, 13.40)	(8.10, 7.59)	(11.95, 11.44)	(4.59, 4.06)	(10.42, 9.90)
			1.5	(3.93, 3.39)	(4.72, 4.19)	(3.40, 2.85)	(4.39, 3.86)	(3.67, 3.13)	(4.05, 3.51)
			2.0	(1.97, 1.38)	(2.61, 2.05)	(2.20, 1.62)	(2.65, 2.09)	(3.16, 2.61)	(2.61, 2.05)
		1.0	1.0	(3.18, 2.64)	(6.77, 6.25)	(1.64, 1.03)	(5.30, 4.77)	(1.26, 0.57)	(3.70, 3.16)
			1.5	(2.32, 1.75)	(3.02, 2.47)	(1.74, 1.14)	(2.64, 2.08)	(1.72, 1.12)	(2.20, 1.63)
			2.0	(1.83, 1.23)	(2.06, 1.47)	(1.67, 1.06)	(1.94, 1.36)	(2.02, 1.43)	(1.80, 1.20)
		1.5	1.0	(1.18, 0.45)	(2.65, 2.09)	(1.01, 0.11)	(1.88, 1.29)	(1.00, 0.04)	(1.19, 0.48)
			1.5	(1.40, 0.75)	(1.81, 1.21)	(1.14, 0.40)	(1.54, 0.91)	(1.14, 0.39)	(1.26, 0.57)
			2.0	(1.47, 0.83)	(1.55, 0.92)	(1.27, 0.59)	(1.42, 0.77)	(1.40, 0.75)	(1.28, 0.60)
		2.0	1.0	(1.00, 0.02)	(1.10, 0.34)	(1.00, 0.00)	(1.01, 0.11)	(1.00, 0.00)	(1.00, 0.00)
			1.5	(1.07, 0.26)	(1.17, 0.45)	(1.01, 0.08)	(1.07, 0.27)	(1.00, 0.07)	(1.01, 0.10)
			2.0	(1.18, 0.46)	(1.20, 0.49)	(1.07, 0.27)	(1.12, 0.36)	(1.11, 0.35)	(1.05, 0.23)
0.7156	3.0	0.0	1.0	(34.97, 34.46)	(20.56, 20.05)	(28.02, 27.52)	(19.30, 18.79)	(50.29, 49.79)	(19.23, 18.72)
			1.5	(6.66, 6.14)	(6.97, 6.45)	(7.80, 7.28)	(7.03, 6.51)	(12.95, 12.44)	(7.18, 6.66)
			2.0	(2.18, 1.60)	(3.57, 3.03)	(3.54, 3.00)	(3.93, 3.39)	(6.79, 6.27)	(4.17, 3.63)
		0.5	1.0	(16.25, 15.74)	(12.92, 12.41)	(9.35, 8.83)	(11.29, 10.78)	(5.45, 4.92)	(10.06, 9.55)
			1.5	(5.37, 4.84)	(5.18, 4.65)	(4.27, 3.74)	(4.79, 4.26)	(4.39, 3.85)	(4.45, 3.92)
			2.0	(2.77, 2.22)	(3.09, 2.54)	(2.88, 2.33)	(3.06, 2.51)	(3.88, 3.34)	(2.99, 2.44)
		1.0	1.0	(3.84, 3.30)	(6.93, 6.41)	(1.74, 1.13)	(5.51, 4.99)	(1.19, 0.47)	(3.98, 3.44)
			1.5	(2.81, 2.25)	(3.41, 2.87)	(1.93, 1.34)	(2.96, 2.40)	(1.71, 1.10)	(2.46, 1.89)
			2.0	(2.30, 1.73)	(2.39, 1.83)	(1.92, 1.33)	(2.21, 1.64)	(2.13, 1.55)	(2.02, 1.43)
		1.5	1.0	(1.14, 0.40)	(2.91, 2.36)	(1.00, 0.05)	(2.05, 1.47)	(1.00, 0.00)	(1.22, 0.51)
			1.5	(1.45, 0.81)	(2.02, 1.44)	(1.11, 0.35)	(1.67, 1.06)	(1.05, 0.24)	(1.31, 0.63)
			2.0	(1.60, 0.98)	(1.73, 1.13)	(1.29, 0.62)	(1.55, 0.92)	(1.32, 0.65)	(1.35, 0.69)
		2.0	1.0	(1.00, 0.00)	(1.12, 0.36)	(1.00, 0.00)	(1.01, 0.09)	(1.00, 0.00)	(1.00, 0.00)
			1.5	(1.03, 0.18)	(1.21, 0.50)	(1.00, 0.02)	(1.07, 0.27)	(1.00, 0.00)	(1.01, 0.07)
			2.0	(1.17, 0.45)	(1.25, 0.56)	(1.04, 0.20)	(1.14, 0.40)	(1.03, 0.17)	(1.05, 0.22)

From Tables 2 and 3, it is found that the in-control performance of the OSPRT chart designed under the Normal model deteriorates rapidly as the skewness increases. For instance, when the skewness increases from zero to $\theta = 1$, the ARL_0 value falls from 370.4 to values ranging from 40 to 80, for both the Gamma and Lognormal distributions (Tables 2 & 3). Similar observations have also been captured for the in-control SDRL ($SDRL_0$) performance, dropping from 369.90 to almost the same range of values as the preceding observation. This is in fact an alarming sign, since the ARL_0 has shrunk by almost 90%, implying that the false alarms are occurring at a rate 10 times as high as the original rate. As the perceived skewness continues to increase (i.e., $\theta = 2, 3$), both the ARL_0 and $SDRL_0$ values shrink further, reaching values as low as 15 for both the Gamma and Lognormal distributions. This can be endangering to the operation of a production line, as excessive false alarms may diminish the confidence of operating personnel (Montgomery 2019).

Referring to the out-of-control performances, one observes a general decline in the (ARL_1, $SDRL_1$) values as compared to those in Table 1, presumably due to the tremendous fall in the ARL_0 values as a result of skewed data distributions. For example, when the skewness increases from zero to $\theta = 1$ for the Gamma distribution, the (ARL_1, $SDRL_1$) values at $(\delta, \eta) = (0.5, 1.0)$ are found to drop from (92.38, 91.88) (Table 1) to (19.96, 19.46) (Table 2), when $(k, \gamma) = (0.1, 4.0)$ have been used. However, there are some exceptions to this observation, specifically for cases with $(k, \gamma) \in \{(0.5, 2.0), (1.0, 2.5)\}$. For instance, when the skewness increases from zero to $\theta = 1$ for the Lognormal distribution, the (ARL_1, $SDRL_1$) values at $(\delta, \eta) = (0.0, 1.5)$ are found to increase from (4.01, 3.48) (Table 1) to (6.75, 6.23) (Table 3), when $(k, \gamma) = (1.0, 2.5)$ have been used. It is interesting to note that, generally, both the ARL_0 and ARL_1 values decrease as data become more positively skewed. This could be explained by the fact that the 'squared' operation in Equation (1) somehow exacerbates the skewed condition, making the control statistic more likely to fall in the out-of-control region. While a decreased ARL_1 might seem to indicate a better detection ability, the worsening in-control performance due to skewed distributions is unacceptable and should not be neglected. In the following section, we will introduce a new method for adjusting the control limits of the OSPRT chart to attain the desired in-control performance.

THE OSPRT CHART WITH SKEWNESS-CORRECTED CONTROL LIMITS

In this section, we outline the steps required to compute the new control limits for the OSPRT chart based on skewness correction. The method involves adjusting both the control limits (i.e., g and h) so that the constraints on ARL_0 and ASN_0 are satisfied under non-Normal conditions. A rough idea of the implementation is as follows: Suppose that the ARL_0 drops from 370.4 to 40 as a result of an increased skewness. This means that observations from the in-control process are now more likely to fall in the rejection region of the OSPRT chart. To regain the desired level of in-control performance, it is necessary to increase the upper control limit h so that the control statistic has a lower chance of falling outside of h, thus pulling up the ARL_0. The same mechanism applies to the adjustment of g in the effort of bringing the ASN_0 back to the desired level.

The step-by-step procedure for adjusting the control limits of the OSPRT chart based on skewness correction is detailed as follows: Step 1: Specify four design specifications, i.e., k, γ, τ, and the desired in-control ASN_0 ($\underline{n}$). Step 2: Initialise the values of g' and h'. We recommend setting the initial values of g' and h' equal to the values of g and h obtained under the full Normal model, respectively. Step 3: Adjust the value of h' to satisfy the constraint $ARL_0 = \tau$ while keeping the value of g' fixed. If the simulated value of ARL_0 is smaller than τ, increase the value of h'; whereas if the simulated value of ARL_0 is larger than τ, reduce the value of h'. Step 4: Adjust the value of g' to satisfy the constraint $ASN_0 = \underline{n}$ while keeping the value of h' fixed. If the simulated value of ASN_0 is larger than $\underline{n}$, increase the value of g'; whereas if the simulated value of ASN_0 is smaller than $\underline{n}$, reduce the value of g'. Step 5: Repeat Steps 3 and 4 until both the values of g' and h' converge.

Upon running these algorithm, we found that the value of h' increases considerably as the level of skewness increases, whereas the value of g' remains rather stable and does not deviate much from the original value g. From this observation, it may be useful to customise the size of increment (or decrement) for each of g' and h' in order to achieve optimum computational efficiency.

Tables 4 and 5 tabulate the adjusted control limits (g', h'), as well as the (ARL, SDRL) performances of the skewness-corrected OSPRT chart, for six combinations of reference parameters $(k, \gamma) \in \{(0.1, 1.5), (0.1, 4.0), (0.5,$

2.0), (0.5, 5.0), (1.0, 2.5), (1.0, 6.0)}. Note that Table 4 shows results for the Gamma distribution with varying shape parameter α, whereas Table 5 shows results for the Lognormal distribution with varying scale parameter σ_{LN}. Skewness correction has been applied to both distributions with respect to three levels of skewness, i.e., $\theta \in \{1.0, 2.0, 3.0\}$. As a numeric example, when $(k, \gamma) = (0.5, 5.0)$ is chosen for Lognormal data with skewness $\theta = 2.0$ (i.e., $\sigma_{LN} = 0.5514$), the corrected control limits are computed as $(g', h') = (-16.840, 48.314)$ (Table 5) using the algorithm detailed in the preceding paragraph. It is worth noting that the (ARL_0, $SDRL_0$) values (= (370.40, 369.90)) of the skewness-corrected OSPRT chart under the Lognormal distribution now resemble those of the original OSPRT chart under the full Normal model (Table 1). The same applies to the Gamma distribution and all other levels of skewness.

TABLE 4. Skewness-corrected control limits (g', h') and the corresponding (ARL, SDRL) values of the OSPRT chart under the Gamma distribution, for $ARL_0 = \tau = 370.4$, $ASN_0 = 5$, $(k, \gamma) \in \{(0.1, 1.5), (0.1, 4.0), (0.5, 2.0), (0.5, 5.0), (1.0, 2.5), (1.0, 6.0)\}$, and $\theta \in \{1.0, 2.0, 3.0\}$

			(k, γ)	(0.1, 1.5)	(0.1, 4.0)	(0.5, 2.0)	(0.5, 5.0)	(1.0, 2.5)	(1.0, 6.0)
				(g', h')	(g', h')	(g', h')	(g', h')	(g', h')	(g', h')
a	θ	δ	η	(ARL, SDRL)	(ARL, SDRL)	(ARL, SDRL)	(ARL, SDRL)	(ARL, SDRL)	(ARL, SDRL)
4.0000	1.0	0.0	1.0	(–1.927, 31.465) (370.40, 369.90)	(–13.431, 17.735) (370.40, 369.90)	(–3.114, 36.300) (370.40, 369.90)	(–16.790, 20.415) (370.34, 369.84)	(–1.880, 58.868) (370.40, 369.90)	(–17.423, 25.894) (370.40, 369.90)
			1.5	(2.63, 2.07)	(17.63, 17.13)	(4.75, 4.22)	(20.02, 19.52)	(6.97, 6.45)	(19.75, 19.24)
			2.0	(1.35, 0.69)	(3.18, 2.64)	(1.66, 1.04)	(4.48, 3.95)	(3.02, 2.47)	(5.03, 4.51)
		0.5	1.0	(30.28, 29.77)	(129.54, 129.04)	(11.71, 11.19)	(112.99, 112.49)	(3.57, 3.03)	(83.85, 83.35)
			1.5	(2.50, 1.94)	(9.42, 8.91)	(2.48, 1.91)	(9.12, 8.61)	(2.82, 2.27)	(7.46, 6.94)
			2.0	(1.44, 0.79)	(2.68, 2.12)	(1.58, 0.96)	(3.01, 2.46)	(2.32, 1.75)	(2.93, 2.38)
		1.0	1.0	(2.49, 1.92)	(31.86, 31.36)	(1.50, 0.87)	(22.13, 21.62)	(1.30, 0.63)	(9.13, 8.62)
			1.5	(1.78, 1.18)	(4.24, 3.71)	(1.51, 0.88)	(3.63, 3.09)	(1.64, 1.03)	(2.58, 2.02)
			2.0	(1.41, 0.75)	(1.96, 1.37)	(1.38, 0.73)	(1.95, 1.36)	(1.77, 1.17)	(1.77, 1.17)
		1.5	1.0	(1.18, 0.46)	(4.49, 3.96)	(1.03, 0.17)	(2.46, 1.89)	(1.02, 0.13)	(1.19, 0.48)
			1.5	(1.31, 0.64)	(1.88, 1.29)	(1.14, 0.40)	(1.57, 0.94)	(1.20, 0.49)	(1.24, 0.55)
			2.0	(1.28, 0.60)	(1.43, 0.79)	(1.20, 0.49)	(1.35, 0.69)	(1.40, 0.75)	(1.24, 0.55)
		2.0	1.0	(1.01, 0.09)	(1.10, 0.33)	(1.00, 0.01)	(1.02, 0.12)	(1.00, 0.00)	(1.00, 0.02)
			1.5	(1.09, 0.31)	(1.15, 0.41)	(1.02, 0.15)	(1.06, 0.26)	(1.04, 0.20)	(1.02, 0.13)
			2.0	(1.15, 0.42)	(1.15, 0.41)	(1.08, 0.29)	(1.10, 0.32)	(1.18, 0.46)	(1.05, 0.24)
1.0000	2.0	0.0	1.0	(–2.091, 57.039) (370.40, 369.90)	(–13.626, 37.099) (370.40, 369.90)	(–3.240, 62.747) (370.40, 369.90)	(–16.656, 40.956) (370.40, 369.90)	(–2.002, 90.972) (370.40, 369.90)	(–17.415, 48.490) (370.40, 369.90)
			1.5	(4.76, 4.23)	(25.05, 24.55)	(8.67, 8.16)	(28.14, 27.64)	(11.86, 11.35)	(28.11, 27.61)

continue to next page

continue from previous page

			2.0	(1.57, 0.94)	(5.46, 4.94)	(2.70, 2.14)	(7.22, 6.70)	(5.10, 4.57)	(7.80, 7.29)
		0.5	1.0	(49.29, 48.79)	(175.16, 174.66)	(19.46, 18.95)	(156.30, 155.80)	(4.52, 3.99)	(121.75, 121.25)
			1.5	(4.34, 3.80)	(15.21, 14.70)	(3.89, 3.35)	(14.66, 14.15)	(3.79, 3.25)	(12.03, 11.52)
			2.0	(2.11, 1.53)	(4.49, 3.95)	(2.43, 1.87)	(4.90, 4.37)	(3.43, 2.88)	(4.61, 4.08)
		1.0	1.0	(3.33, 2.79)	(57.76, 57.25)	(1.68, 1.06)	(41.18, 40.67)	(1.22, 0.51)	(17.09, 16.58)
			1.5	(2.47, 1.90)	(7.17, 6.65)	(1.84, 1.25)	(6.02, 5.50)	(1.70, 1.09)	(3.91, 3.37)
			2.0	(2.04, 1.45)	(3.09, 2.54)	(1.83, 1.23)	(2.95, 2.40)	(2.10, 1.52)	(2.48, 1.91)
		1.5	1.0	(1.15, 0.42)	(8.35, 7.84)	(1.00, 0.06)	(3.88, 3.34)	(1.00, 0.00)	(1.28, 0.60)
			1.5	(1.45, 0.81)	(2.74, 2.18)	(1.14, 0.40)	(2.09, 1.51)	(1.07, 0.28)	(1.39, 0.74)
			2.0	(1.57, 0.95)	(1.94, 1.35)	(1.32, 0.65)	(1.74, 1.13)	(1.35, 0.69)	(1.43, 0.79)
		2.0	1.0	(1.00, 0.00)	(1.14, 0.40)	(1.00, 0.00)	(1.01, 0.12)	(1.00, 0.00)	(1.00, 0.00)
			1.5	(1.04, 0.20)	(1.25, 0.56)	(1.00, 0.02)	(1.10, 0.33)	(1.00, 0.00)	(1.01, 0.11)
			2.0	(1.20, 0.49)	(1.30, 0.62)	(1.05, 0.24)	(1.18, 0.46)	(1.03, 0.19)	(1.07, 0.27)
0.4444	3.0	0.0	1.0	(–2.298, 87.099) (370.40, 369.90)	(–13.516, 60.378) (370.40, 369.90)	(–3.350, 93.100) (370.40, 369.90)	(–16.555, 65.286) (370.40, 369.90)	(–2.168, 125.501) (370.40, 369.90)	(–17.354, 74.624) (370.40, 369.90)
			1.5	(8.42, 7.90)	(33.14, 32.63)	(14.37, 13.86)	(36.00, 35.49)	(17.61, 17.11)	(36.80, 36.29)
			2.0	(2.59, 2.03)	(8.37, 7.85)	(4.55, 4.02)	(10.53, 10.02)	(8.32, 7.80)	(11.46, 10.95)
		0.5	1.0	(71.86, 71.36)	(207.60, 207.10)	(28.48, 27.98)	(187.13, 186.63)	(5.29, 4.77)	(150.68, 150.18)
			1.5	(6.67, 6.15)	(21.57, 21.06)	(5.69, 5.16)	(20.82, 20.31)	(4.59, 4.05)	(17.18, 16.68)
			2.0	(3.48, 2.94)	(6.94, 6.42)	(3.68, 3.14)	(7.24, 6.72)	(4.45, 3.92)	(6.73, 6.21)
		1.0	1.0	(4.22, 3.68)	(82.81, 82.31)	(1.83, 1.23)	(60.24, 59.74)	(1.07, 0.28)	(26.49, 25.98)
			1.5	(3.18, 2.63)	(10.83, 10.32)	(2.12, 1.54)	(9.02, 8.50)	(1.63, 1.02)	(5.60, 5.07)
			2.0	(2.76, 2.20)	(4.60, 4.07)	(2.26, 1.68)	(4.28, 3.74)	(1.99, 1.40)	(3.37, 2.83)
		1.5	1.0	(1.06, 0.26)	(13.50, 12.99)	(1.00, 0.00)	(5.63, 5.10)	(1.00, 0.00)	(1.35, 0.69)
			1.5	(1.43, 0.79)	(3.87, 3.34)	(1.07, 0.27)	(2.72, 2.17)	(1.00, 0.00)	(1.53, 0.90)
			2.0	(1.77, 1.17)	(2.63, 2.07)	(1.31, 0.64)	(2.21, 1.63)	(1.14, 0.40)	(1.63, 1.01)
		2.0	1.0	(1.00, 0.00)	(1.18, 0.46)	(1.00, 0.00)	(1.01, 0.09)	(1.00, 0.00)	(1.00, 0.00)
			1.5	(1.00, 0.00)	(1.35, 0.69)	(1.00, 0.00)	(1.11, 0.35)	(1.00, 0.00)	(1.00, 0.05)
			2.0	(1.10, 0.32)	(1.46, 0.82)	(1.00, 0.03)	(1.24, 0.55)	(1.00, 0.00)	(1.06, 0.24)

TABLE 5. Skewness-corrected control limits (g', h') and the corresponding (ARL, SDRL) values of the OSPRT chart under the Lognormal distribution, for $ARL_0 = \tau = 370.4$, $ASN_0 = 5$, $(k, \gamma) \in \{(0.1, 1.5), (0.1, 4.0), (0.5, 2.0), (0.5, 5.0), (1.0, 2.5), (1.0, 6.0)\}$, and $\theta \in \{1.0, 2.0, 3.0\}$

			(k, γ)	(0.1, 1.5)	(0.1, 4.0)	(0.5, 2.0)	(0.5, 5.0)	(1.0, 2.5)	(1.0, 6.0)
				(g', h')	(g', h')	(g', h')	(g', h')	(g', h')	(g', h')
σ_{LN}	θ	δ	η	(ARL, SDRL)	(ARL, SDRL)	(ARL, SDRL)	(ARL, SDRL)	(ARL, SDRL)	(ARL, SDRL)
0.3143	1.0	0.0	1.0	(–1.939, 33.862) (370.40, 369.90)	(–13.438, 19.931) (370.40, 369.90)	(–3.136, 38.611) (370.40, 369.90)	(–16.815, 22.706) (370.40, 369.90)	(–1.888, 60.934) (370.40, 369.90)	(–17.420, 28.367) (370.40, 369.90)
			1.5	(2.72, 2.16)	(20.20, 19.69)	(4.89, 4.36)	(22.96, 22.45)	(6.99, 6.47)	(22.61, 22.10)
			2.0	(1.37, 0.72)	(3.41, 2.87)	(1.67, 1.06)	(4.88, 4.35)	(2.98, 2.43)	(5.49, 4.96)
		0.5	1.0	(33.72, 33.22)	(146.19, 145.69)	(12.52, 12.01)	(127.72, 127.22)	(3.52, 2.98)	(96.06, 95.56)
			1.5	(2.50, 1.93)	(10.84, 10.33)	(2.45, 1.88)	(10.45, 9.94)	(2.75, 2.19)	(8.40, 7.88)
			2.0	(1.45, 0.81)	(2.83, 2.28)	(1.57, 0.94)	(3.20, 2.65)	(2.25, 1.68)	(3.09, 2.54)
		1.0	1.0	(2.46, 1.89)	(38.81, 38.31)	(1.48, 0.84)	(26.66, 26.16)	(1.29, 0.61)	(10.55, 10.04)
			1.5	(1.75, 1.14)	(4.69, 4.16)	(1.48, 0.84)	(3.95, 3.41)	(1.61, 0.99)	(2.70, 2.14)
			2.0	(1.39, 0.74)	(2.01, 1.43)	(1.35, 0.69)	(2.00, 1.41)	(1.71, 1.11)	(1.79, 1.19)
		1.5	1.0	(1.17, 0.45)	(5.06, 4.54)	(1.03, 0.17)	(2.61, 2.05)	(1.02, 0.15)	(1.19, 0.48)
			1.5	(1.28, 0.60)	(1.93, 1.34)	(1.13, 0.38)	(1.59, 0.96)	(1.20, 0.48)	(1.24, 0.54)
			2.0	(1.26, 0.57)	(1.43, 0.78)	(1.18, 0.46)	(1.35, 0.69)	(1.37, 0.71)	(1.23, 0.53)
		2.0	1.0	(1.01, 0.09)	(1.10, 0.33)	(1.00, 0.01)	(1.01, 0.12)	(1.00, 0.01)	(1.00, 0.02)
			1.5	(1.08, 0.29)	(1.14, 0.40)	(1.02, 0.15)	(1.06, 0.25)	(1.05, 0.22)	(1.02, 0.13)
			2.0	(1.13, 0.39)	(1.14, 0.39)	(1.07, 0.27)	(1.09, 0.31)	(1.17, 0.45)	(1.05, 0.23)
0.5514	2.0	0.0	1.0	(–2.099, 63.508) (370.40, 369.90)	(–13.634, 44.192) (370.40, 369.90)	(–3.303, 69.182) (370.40, 369.90)	(–16.840, 48.314) (370.40, 369.90)	(–2.029, 96.178) (370.40, 369.90)	(–17.458, 56.164) (370.40, 369.90)
			1.5	(4.61, 4.08)	(33.53, 33.02)	(8.85, 8.33)	(37.51, 37.01)	(11.37, 10.86)	(37.20, 36.70)
			2.0	(1.57, 0.94)	(6.40, 5.88)	(2.42, 1.86)	(8.77, 8.26)	(4.54, 4.01)	(9.55, 9.04)
		0.5	1.0	(60.19, 59.69)	(207.32, 206.82)	(21.80, 21.30)	(185.53, 185.03)	(4.25, 3.71)	(149.25, 148.75)
			1.5	(3.95, 3.42)	(20.43, 19.93)	(3.57, 3.03)	(19.57, 19.07)	(3.43, 2.89)	(15.64, 15.13)
			2.0	(1.88, 1.29)	(5.06, 4.53)	(2.13, 1.56)	(5.60, 5.07)	(2.95, 2.40)	(5.13, 4.60)
		1.0	1.0	(3.12, 2.57)	(79.63, 79.13)	(1.58, 0.96)	(56.95, 56.45)	(1.20, 0.50)	(23.09, 22.59)
			1.5	(2.24, 1.67)	(8.96, 8.45)	(1.69, 1.08)	(7.27, 6.75)	(1.62, 1.00)	(4.30, 3.77)
			2.0	(1.76, 1.15)	(3.21, 2.66)	(1.62, 1.00)	(3.06, 2.51)	(1.91, 1.31)	(2.48, 1.91)
		1.5	1.0	(1.14, 0.40)	(10.90, 10.39)	(1.01, 0.09)	(4.38, 3.85)	(1.00, 0.03)	(1.26, 0.57)
			1.5	(1.36, 0.70)	(2.84, 2.29)	(1.12, 0.37)	(2.08, 1.50)	(1.10, 0.33)	(1.35, 0.68)
			2.0	(1.42, 0.78)	(1.87, 1.28)	(1.24, 0.55)	(1.66, 1.05)	(1.34, 0.67)	(1.37, 0.72)

continue to next page

continue from previous page

		2.0	1.0	(1.00, 0.01)	(1.13, 0.38)	(1.00, 0.00)	(1.01, 0.11)	(1.00, 0.00)	(1.00, 0.00)
			1.5	(1.05, 0.23)	(1.21, 0.51)	(1.00, 0.07)	(1.08, 0.29)	(1.00, 0.05)	(1.01, 0.11)
			2.0	(1.16, 0.43)	(1.24, 0.54)	(1.06, 0.24)	(1.14, 0.40)	(1.08, 0.29)	(1.06, 0.24)
				(–2.290, 93.184)	(–13.845, 69.527)	(–3.468, 99.580)	(–16.956, 74.737)	(–2.155, 129.500)	(–17.485, 84.274)
0.7156	3.0	0.0	1.0	(370.40, 369.90)	(370.40, 369.90)	(370.40, 369.90)	(370.40, 369.90)	(370.40, 369.90)	(370.40, 369.90)
			1.5	(7.50, 6.98)	(45.34, 44.84)	(13.50, 12.99)	(50.70, 50.20)	(13.72, 13.21)	(50.89, 50.39)
			2.0	(1.98, 1.40)	(9.89, 9.38)	(3.50, 2.95)	(13.14, 12.63)	(5.89, 5.37)	(14.08, 13.57)
		0.5	1.0	(85.60, 85.10)	(238.49, 237.99)	(31.04, 30.53)	(216.62, 216.12)	(4.46, 3.93)	(180.79, 180.29)
			1.5	(5.65, 5.12)	(30.14, 29.63)	(4.68, 4.15)	(28.96, 28.46)	(3.99, 3.46)	(23.43, 22.92)
			2.0	(2.53, 1.97)	(7.72, 7.20)	(2.74, 2.18)	(8.41, 7.90)	(3.70, 3.16)	(7.52, 7.00)
		1.0	1.0	(3.65, 3.11)	(110.02, 109.52)	(1.63, 1.01)	(81.93, 81.43)	(1.15, 0.42)	(36.42, 35.92)
			1.5	(2.64, 2.08)	(13.87, 13.36)	(1.81, 1.21)	(11.15, 10.64)	(1.60, 0.98)	(6.15, 5.63)
			2.0	(2.13, 1.55)	(4.61, 4.08)	(1.81, 1.21)	(4.28, 3.75)	(2.09, 1.51)	(3.21, 2.66)
		1.5	1.0	(1.09, 0.31)	(17.81, 17.30)	(1.00, 0.03)	(6.42, 5.90)	(1.00, 0.00)	(1.30, 0.62)
			1.5	(1.35, 0.69)	(3.82, 3.28)	(1.08, 0.30)	(2.56, 2.00)	(1.02, 0.14)	(1.43, 0.78)
			2.0	(1.51, 0.87)	(2.32, 1.75)	(1.24, 0.54)	(1.96, 1.37)	(1.25, 0.55)	(1.48, 0.85)
		2.0	1.0	(1.00, 0.00)	(1.14, 0.39)	(1.00, 0.00)	(1.01, 0.09)	(1.00, 0.00)	(1.00, 0.00)
			1.5	(1.02, 0.12)	(1.26, 0.57)	(1.00, 0.01)	(1.08, 0.30)	(1.00, 0.00)	(1.01, 0.07)
			2.0	(1.12, 0.37)	(1.31, 0.64)	(1.02, 0.16)	(1.17, 0.44)	(1.00, 0.04)	(1.05, 0.23)

From Tables 4 and 5, it is clear that the value of h' increases as θ increases, whereas the value of g' does not differ too much despite the increase in skewness. In fact, if we observe closely enough, it appears that h' follows a superlinear growth trend in response to an increase in θ, i.e., h' rises at an increasing rate as θ increases. For example, when $(k, \gamma) = (0.5, 2.0)$ is chosen for the Gamma distribution, increasing the skewness from 1.0 to 2.0 causes h' to rise from 36.300 to 62.747 (i.e., an increment of 26.447), whereas increasing the skewness from 2.0 to 3.0 causes h' to rise further from 62.747 to 93.100 (i.e., an increment of 30.353) (Table 4). Figures 1 and 2 show the movements of g' and h' as the degree of skewness increases from 0.0 through 3.0 for the Gamma and Lognormal distributions, respectively. From both figures, it is quite clear that h' is an increasing function of θ. All six curves exhibit a slightly convex shape, and all of them have rather similar 'slopes'. On the other hand, there is very little we can deduce about g', since there is no particularly interesting trend based on the graphs, and the value of g' relies on the choice of (k, γ).

Referring to the out-of-control performances, it is found that the OSPRT chart loses part of its detection ability upon skewness correction. In particular, it is noticed that the skewness-corrected OSPRT chart becomes less sensitive to small and moderate process shifts compared to their uncorrected versions, made worse when the degree of skewness increases. For instance, when $(k, \gamma) = (1.0, 6.0)$ is chosen for the Gamma distribution with skewness $\theta = 1.0$ (i.e., $\alpha = 4$), the uncorrected OSPRT chart yields $(ARL_1, SDRL_1) = (3.66, 3.12)$ at $(\delta, \eta) = (0.5, 1.5)$ (Table 2), whereas the skewness-corrected OSPRT chart yields (ARL_1, $SDRL_1$) = (7.46, 6.94) (Table 4), which is approximately two times greater than the original value (Tables 2 and 4). In fact, the deterioration in the out-of-control performances is very much anticipated, since the upper control limit of the OSPRT chart has been inflated to guarantee that the ARL_0 value meets the recommended level. For large shift sizes, i.e., $\delta \geq 1.5$ and $\eta \geq 1.5$, the majority of the (ARL_1, $SDRL_1$) values are reasonably close to one, hence skewness correction poses very little influence on the out-of-control performances of the OSPRT chart. It is perhaps interesting to note that the OSPRT chart with combinations $(k, \gamma) \in \{(0.1, 1.5), (0.5, 2.0), (1.0, 2.5)\}$ is very robust towards skewness corrections, especially when the degree of skewness is small. For instance, when the Gamma and Lognormal distributions with skewness $\theta = 1.0$ are

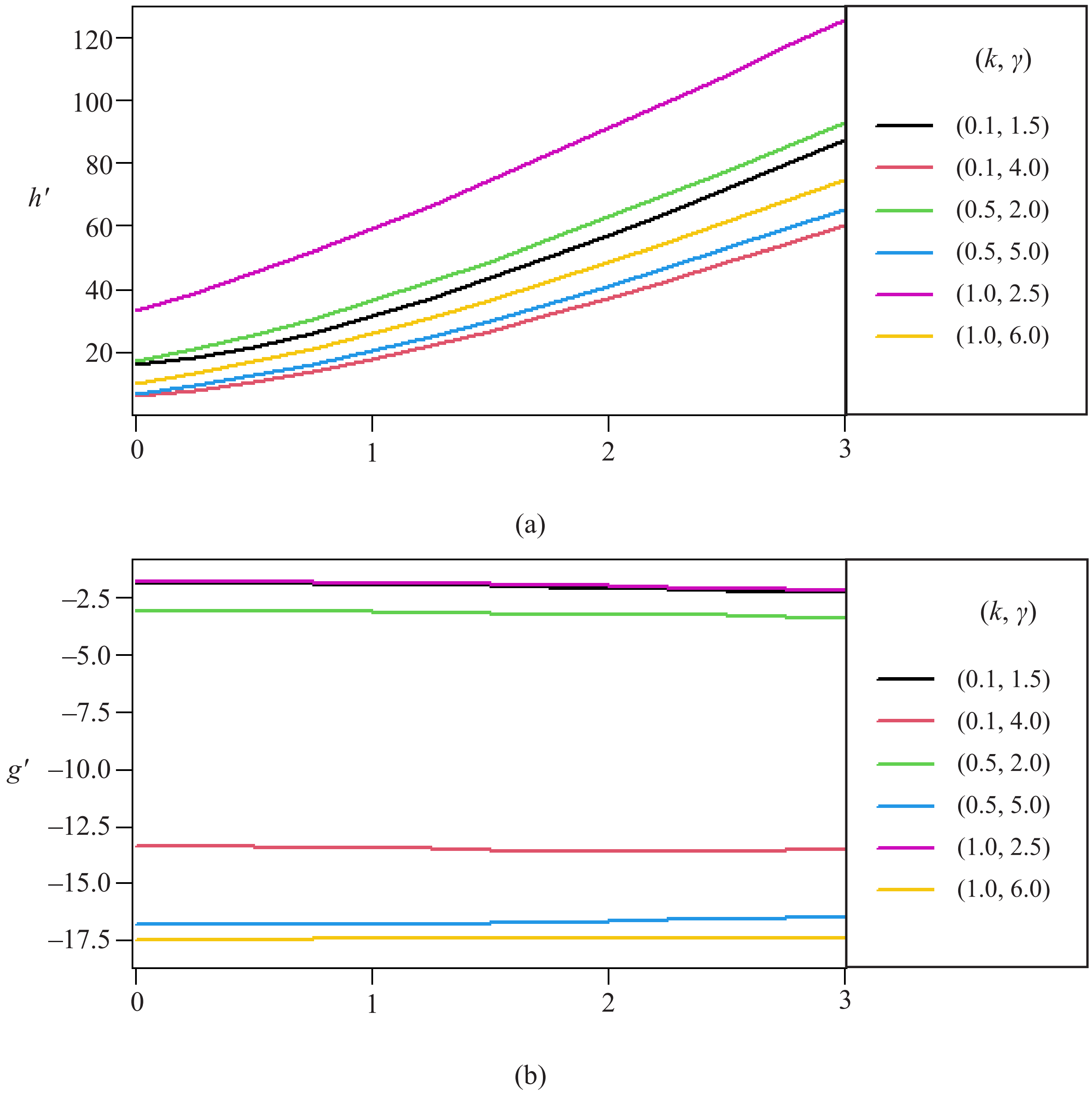

FIGURE 1. Plots of (a) h' and (b) g' versus θ for the OSPRT chart with $(k, \gamma) \in \{(0.1, 1.5),$ $(0.1, 4.0), (0.5, 2.0), (0.5, 5.0), (1.0, 2.5), (1.0, 6.0)\}$ under the Gamma distribution

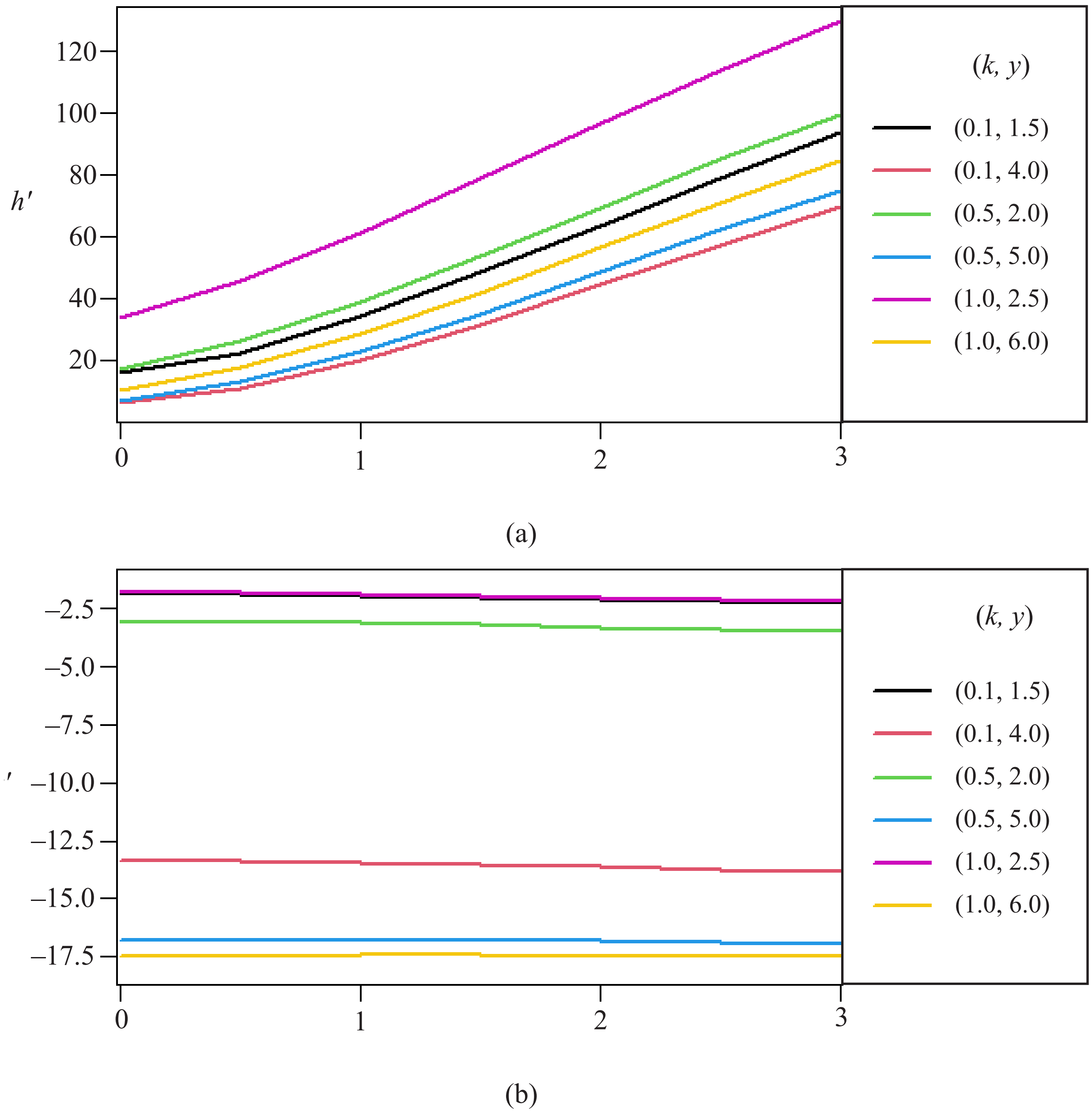

FIGURE 2. Plots of (a) h' and (b) g' versus θ for the OSPRT chart with $(k, \gamma) \in \{(0.1, 1.5), (0.1, 4.0), (0.5, 2.0), (0.5, 5.0), (1.0, 2.5), (1.0, 6.0)\}$ under the Lognormal distribution

considered, the (ARL_1, $SDRL_1$) values of the skewness-corrected OSPRT chart are very close to those of the unadjusted OSPRT chart for all sizes of process shifts, except when $(\delta, \eta) = (0.5, 1.0)$. This observation shows some important information that will help us locate the range of values of (k, γ) such that the performance of the skewness-corrected OSPRT chart can be optimised.

Figures 3 and 4 display the contour plots of the ARL_1 values as a function of k and γ for various combinations of mean and standard deviation shift sizes, i.e., $(\delta, \eta) \in \{(0.5, 1.5), (0.5, 2.0), (1.0, 1.5), (1.0, 2.0), (2.0, 1.5), (2.0, 2.0)\}$, when the Gamma and Lognormal distributions are assumed, respectively. Here, we consider a rectangular domain $(k, \gamma) \in [0.1, 1.0] \times [1.5,$

6.0], which is consistent with the six combinations of (k, γ) chosen in Tables 1 to 5. The colour palette used in our contour plots is taken from a colour map that runs from yellow, green, olive, blue, to black, installed from an R package. It is worth noting that the regions coloured in yellow correspond to locations where the smallest ARL_1 value lies, whereas the regions coloured in black correspond to locations with the largest (or undefined) ARL_1 value. For example, referring to Figure 3(a), the minimum ARL_1 value of the skewness-corrected OSPRT chart under the Gamma distribution seems to be achieved around $k \approx 0.6$ and $\gamma \approx 2.0$ when the shift sizes are (δ, η) = (0.5, 1.5). Note that we only discuss the optimum regions of the skewness-corrected OSPRT chart for θ = 1.0, as the results for θ = 2.0 and 3.0 would be almost similar. Also, when large values of k (e.g., k = 1.0) are used, small values of γ (e.g., γ = 1.0) tend to distort the computation process of the control limits, hence resulting in undefined values of ARL_1 (Figures 3 & 4). Therefore, the bottom right region of each subplot is found to be coloured in black, since the ARL_1 values of those regions cannot be evaluated properly.

From both Figures 3 and 4, it is noticed that different combinations of shift sizes tend to have different regions of optimum performance. For instance, when (δ, η) = (0.5, 1.5), the minimum ARL_1 is achieved somewhere within the elliptical region centred at $k \approx 0.6$ and $\gamma \approx 2.0$ (Figures 3(a) & 4(a)). When (δ, η) = (1.0, 1.5), the minimum ARL_1 is achieved somewhere within the elliptical region centred at $k \approx 0.9$ and $\gamma \approx 3.0$ (Figures 3(c) and 4(c)). Recall that, under the usual Normal distribution, Teoh et al. (2023) suggested setting the reference parameters k and γ equal to Equations (2) and (3), respectively, to achieve an optimum ARL_1 performance for any deterministic shift size (δ, η). When (δ, η) = (0.5, 1.5), the suggested reference parameters (k, γ) for the Normal distribution are (0.400, 1.820), which is arguably close to the location explored via the contour plots for the Weibull and Lognormal distributions. When (δ, η) = (1.0, 1.5), the suggested reference parameters (k, γ) for the Normal distribution are (0.800, 2.900), which is also quite close to the optimum combination found in the contour plots. To this end, it seems that Equations (2) and (3) might be appropriate starting points for exploring the optimal combination (k, γ) that achieves the smallest ARL_1 value. In future, it would be possible to develop a full optimisation algorithm for searching the optimal charting parameters (k, γ, g', h') that minimizes the ARL_1 value for any deterministic shift sizes (δ, η).

AN ILLUSTRATIVE EXAMPLE

In this section, we illustrate an application of our proposed skewness-corrected OSPRT chart for monitoring the weights of radial tyres installed in heavy-duty trucks. A radial tyre is made up of a few components, i.e., tread, sidewall, belt package, carcass, inner liner, bead, and cap plies. These components work together to provide the tyre with its overall performance characteristics, including load-carrying capacity, durability, fuel efficiency, traction, and resistance to wear and damage. During the production of radial tyres, it is crucial that the tyre weights are measured and controlled within certain thresholds to prevent environmental issues (Lee et al., 2022). Past data have suggested that tyre weights follow a Gamma distribution with shape parameter $\alpha = 4$ and rate parameter $\beta = 1$. As the degree of skewness equals one, we shall apply the skewness-corrected OSPRT chart for the Gamma distribution with $\theta = 1.0$ quoted directly from Table 4.

To demonstrate the implementation of the OSPRT chart, we first compute the in-control mean μ_0^* and standard deviation σ_0^* of the tyre weights. The in-control mean μ_0^* is calculated as 4/1 = 4 and the standard deviation σ_0^* is calculated as $\sqrt{4/1^2}$ = 2. Note that all measurements are expressed in units of 10 kilograms (kg), i.e., the mean is 40 kg and the standard deviation is 20 kg. In our illustration, we choose the OSPRT chart with reference parameters (k, γ) = (0.5, 2.0), and the skewness-corrected control limits are (g', h') = (–3.114, 36.300) (Table 4). The control statistic of the skewness-adjusted OSPRT chart is then calculated recursively using Equation (1).

Figure 5 shows the implementation of the skewness-corrected OSPRT chart for monitoring simulated tyre weights data. Suppose that during the vulcanisation process, the heating temperature is incorrectly adjusted, leading to an increase in the mean and variability of the tyre weights by δ = 0.5 and η = 1.5, i.e., the mean and standard deviation of the tyre weights increase to 50 kg and 30 kg, respectively. From Figure 5, it is found that the first six samples result in an in-control decision for the OSPRT chart. In the seventh sample, the control statistic $C_{i,j}$ quickly rises above the upper control limit h' after three consecutive measurements are sought. The control engineer is immediately notified about the shift, and the root cause of the issue is swiftly addressed to bring the process back to normal. The out-of-control run length measured from the start of process monitoring is reported as 7.

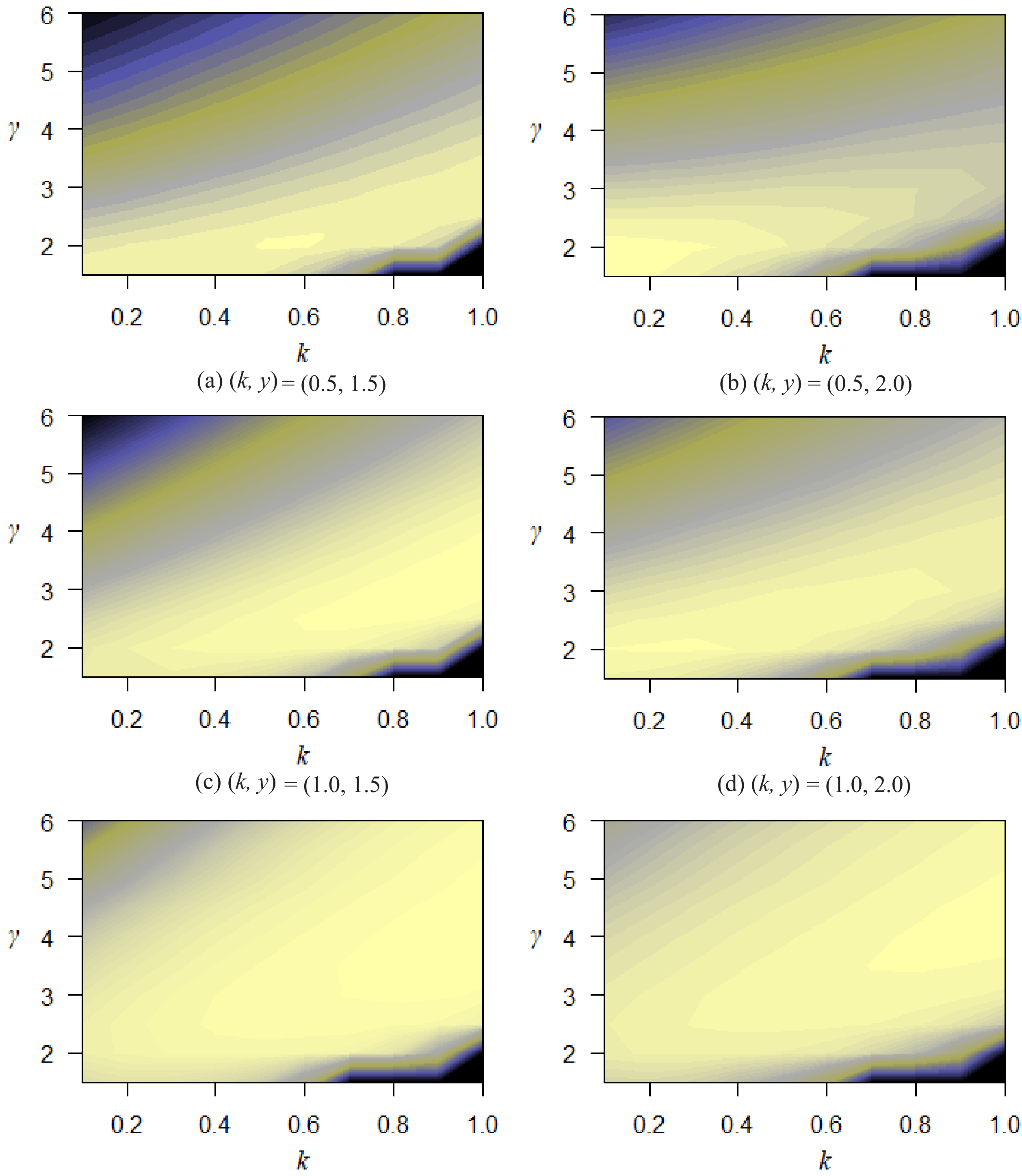

(a) $(k, y) = (0.5, 1.5)$ (b) $(k, y) = (0.5, 2.0)$

(c) $(k, y) = (1.0, 1.5)$ (d) $(k, y) = (1.0, 2.0)$

(e) $(k, y) = (2.0, 1.5)$ (f) $(k, y) = (2.0, 2.0)$

FIGURE 3. Contour plots of the ARL_1 values as a two-dimensional function of k and γ for $(\delta, \eta) \in \{$(a) (0.5, 1.5), (b) (0.5, 2.0), (c) (1.0, 1.5), (d) (1.0, 2.0), (e) (2.0, 1.5), (f) (2.0, 2.0)$\}$ when the Gamma distribution with $\theta = 1.0$ is assumed

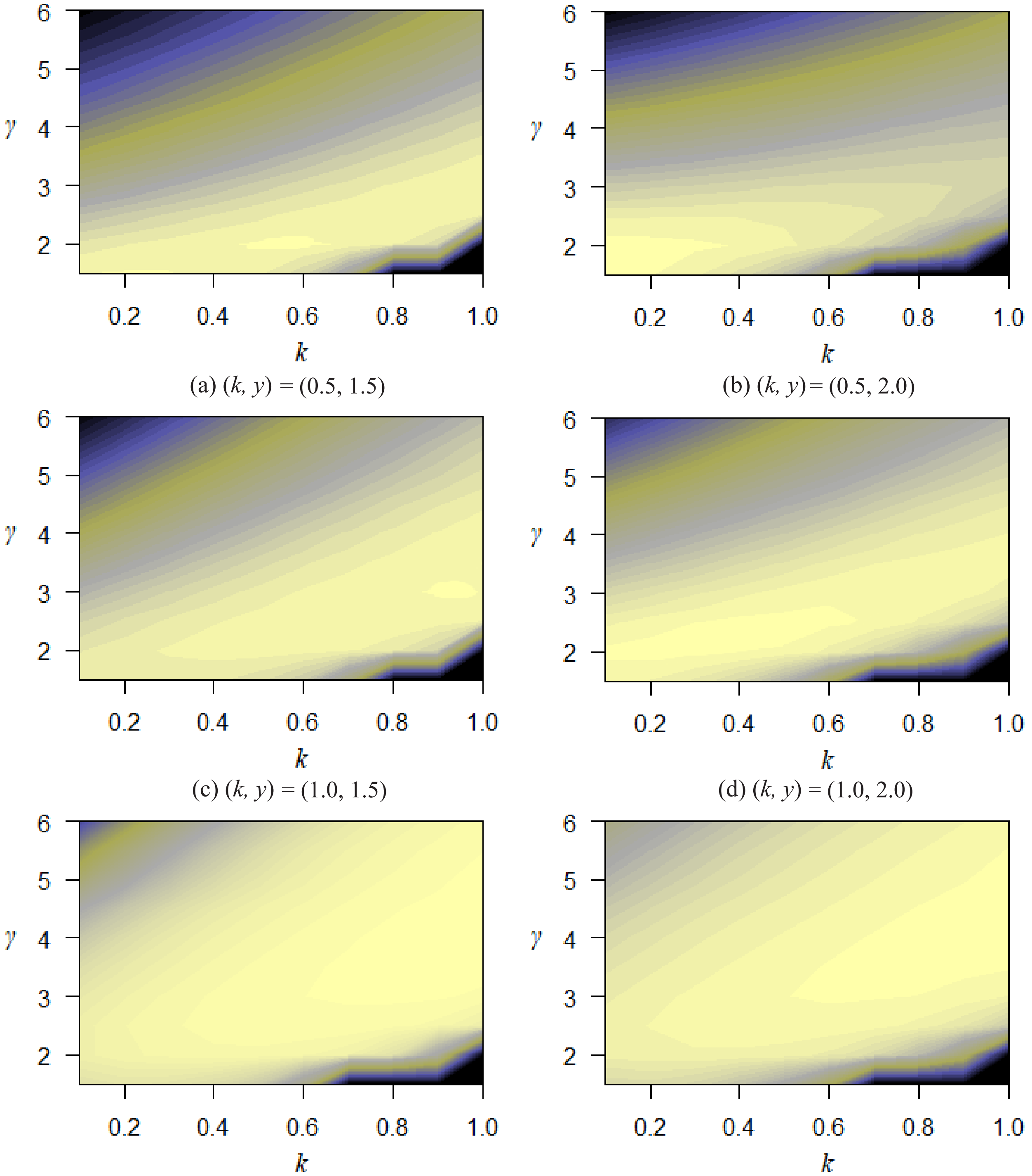

(a) $(k, y) = (0.5, 1.5)$

(b) $(k, y) = (0.5, 2.0)$

(c) $(k, y) = (1.0, 1.5)$

(d) $(k, y) = (1.0, 2.0)$

(e) $(k, y) = (2.0, 1.5)$

(f) $(k, y) = (2.0, 2.0)$

FIGURE 4. Contour plots of the ARL_1 values as a two-dimensional function of k and γ for $(\delta, \eta) \in \{$(a) (0.5, 1.5), (b) (0.5, 2.0), (c) (1.0, 1.5), (d) (1.0, 2.0), (e) (2.0, 1.5), (f) (2.0, 2.0)$\}$ when the Lognormal distribution with $\theta = 1.0$ is assumed

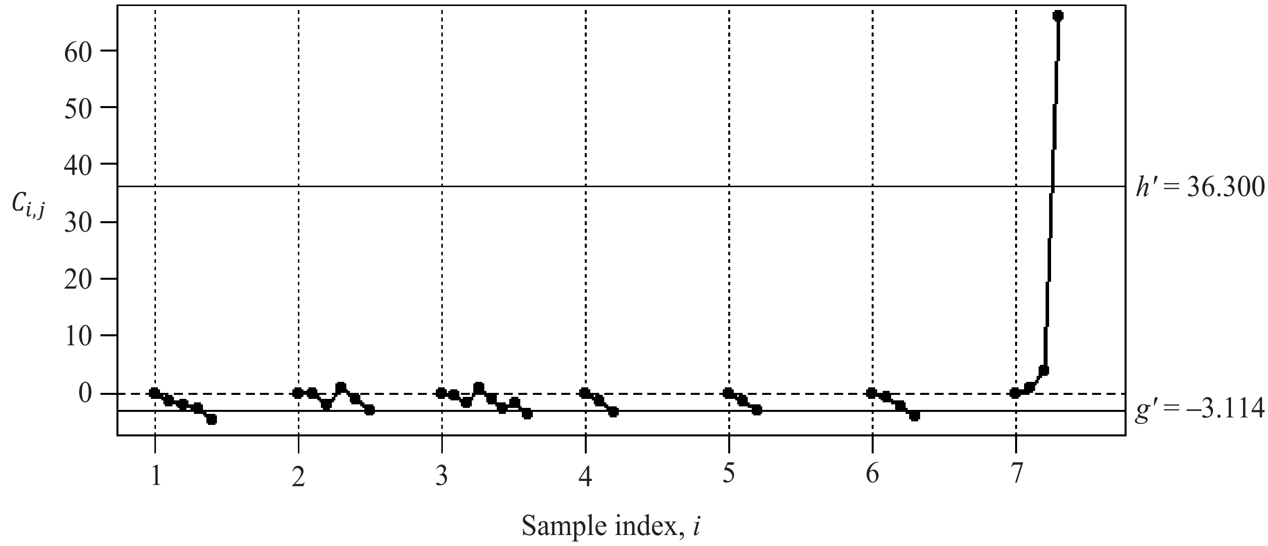

FIGURE 5. The skewness-corrected OSPRT control chart for detecting a joint shift in the mean and variability of tyre weights

Conclusions

This paper discusses the implications of skewness on the performances of the OSPRT chart designed under the Normal model. We have chosen the Gamma and Lognormal distributions in our study as both distributions well describe the behaviours of many industrial and non-industrial processes in the real world, such as product lifetimes, economic indices, and air pollution levels.

Our findings have shown that the OSPRT chart designed under the Normal model performs poorly when the underlying data have a skewed distribution. In particular, the ARL_0 value can shrink to around 10% of its recommended value when the degree of skewness is large. This leads to excessive false alarms during quality applications, which may in turn destroy the inspectors' confidence. As a means of reversing the situation, we propose a robust design for the OSPRT chart based on skewness correction. The method involves modifying the control limits of the OSPRT chart so that the in-control metrics (i.e., ARL_0 and ASN_0) can be brought back to the desired levels. Results show that the skewness-corrected OSPRT chart achieves the desired level of in-control performance, with an acceptable level of deterioration in its out-of-control performances for moderate and large process shift sizes. It is also found that the combinations $(k, \gamma) \in \{(0.1, 1.5), (0.5, 2.0), (1.0, 2.5)\}$ are more robust towards high skewness compared to other combinations of (k, γ). Besides, we also provide some insights into choosing the most appropriate combination of (k, γ) in response to different shift sizes in practice. While the insights gained can be related to the optimality property stated in Teoh et al. (2023), the full optimisation algorithms for searching the optimal (k, γ) specific to the Gamma and Lognormal distributions are still pending.

In future, researchers are highly encouraged to develop new optimisation algorithms for computing the optimal combination of (k, γ) tailored to specific skewed distributions. Alternatively, researchers may derive new charting statistics for the OSPRT chart under the Gamma or Lognormal distributions, but should keep in mind that expressions of such may be extremely convoluted, if not intractable. Another possible direction is through inventing a nonparametric OSPRT chart. Although nonparametric control charts possess the advantage of robustness towards various skewed distributions, they might be less powerful than parametric control charts for the Gamma or Lognormal distributions.

Acknowledgements

This work was supported by the Ministry of Higher Education (MOHE), Malaysia under the Fundamental Research Grant Scheme (FRGS), no. FRGS/1/2021/STG06/HWUM/02/1.

REFERENCES

Abd Razak, N., Zubairi, Y.Z. & Yunus, R.M. 2014. Imputing missing values in modelling the PM10 concentrations. *Sains Malaysiana* 43(10): 1599-1607.

Abu-Shawiesh, M.O. & Abdullah, M.B. 2001. A modified nonparametric univariate control chart for location based on the trimmed mean. *Sains Malaysiana* 30(1): 87-106.

Chowdhury, S., Mukherjee, A. & Chakraborti, S. 2015. Distribution-free phase II CUSUM control chart for joint monitoring of location and scale. *Quality and Reliability Engineering International* 31(1): 135-151.

Dakhn, L.N.B., Bakar, M.A.A. & Ibrahim, K. 2023. Bayesian estimation of time to failure distributions based on skew normal degradation model: An application to GaAs laser degradation data. *Sains Malaysiana* 52(2): 641-653.

Diaz Pulido, A.J., Cordero Franco, A.E. & Tercero Gómez, V.G. 2023. A distribution-free control chart for joint monitoring of location and scale in finite horizon productions. *Computational Statistics* https://doi.org/10.1007/s00180-023-01361-5

Farouk, M., Aziz, N. & Zain, Z. 2020. The application of lognormal distribution on the new two-sided group chain sampling plan. *Sains Malaysiana* 49(5): 1145-1152.

Godase, D.G., Mahadik, S.B. & Rakitzis, A.C. 2022. The SPRT control charts for the Maxwell distribution. *Quality and Reliability Engineering International* 38(4): 1713-1728.

Haq, A., Brown, J. & Moltchanova, E. 2015. An improved maximum exponentially weighted moving average control chart for monitoring process mean and variability. *Quality and Reliability Engineering International* 31(2): 265-290.

Ho, Y.C., Kao, S.C. & Chou, C.F. 2021. Robustness of dispersion control charts in skewed distributions. *International Journal of Industrial Engineering* 28(4): 372-389.

Hossain, M.P., Omar, M.H., Riaz, M. & Arafat, S.Y. 2022. On designing a new control chart for Rayleigh distributed processes with an application to monitor glass fiber strength. *Communications in Statistics-Simulation and Computation* 51(6): 3168-3184.

Hou, S. & Yu, K. 2021. A non-parametric CUSUM control chart for process distribution change detection and change type diagnosis. *International Journal of Production Research* 59(4): 1166-1186.

Huberts, L.C., Schoonhoven, M., Goedhart, R., Diko, M.D. & Does, R.J. 2018. The performance of control charts for large non-normally distributed datasets. *Quality and Reliability Engineering International* 34(6): 979-996.

Khoo, M.B.C. 2004. An extension for the univariate exponentially weighted moving average control chart. *MATEMATIKA* 20(1): 43-48.

Lee, P.H., Torng, C.C., Lin, C.H. & Chou, C.Y. 2022. Control chart pattern recognition using spectral clustering technique and support vector machine under gamma distribution. *Computers & Industrial Engineering* 171(9): 108437.

Li, S.Y., Tang, L.C. & Ng, S.H. 2010. Nonparametric CUSUM and EWMA control charts for detecting mean shifts. *Journal of Quality Technology* 42(2): 209-226.

Mahadik, S.B. & Godase, D.G. 2023. The SPRT sign chart for process location. *Communications in Statistics-Theory and Methods* 52(7): 2276-2290.

Mehmood, R., Lee, M.H., Afzel, A., Bashir, S. & Riaz, M. 2020. Generalized skewness correction structure of $\bar{X}$ control chart for unknown process parameters and skewed probability distributions. *Journal of Statistical Computation and Simulation* 90(8): 1349-1372.

Montgomery, D.C. 2019. *Introduction to Statistical Quality Control*. 8th ed. New York: John Wiley & Sons.

Nawaz, M.S., Azam, M. & Aslam, M. 2021. EWMA and DEWMA repetitive control charts under non-normal processes. *Journal of Applied Statistics* 48(1): 4-40.

Noorossana, R., Fathizadan, S. & Nayebpour, M.R. 2016. EWMA control chart performance with estimated parameters under non-normality. *Quality and Reliability Engineering International* 32(5): 1637-1654.

Qiu, P. 2018. Some perspectives on nonparametric statistical process control. *Journal of Quality Technology* 50(1): 49-65.

Riaz, M., Mehmood, R., Iqbal, M.R. & Abbasi, S.A. 2016. On efficient skewness correction charts under contamination and non-normality. *Quality and Reliability Engineering International* 32(3): 837-854.

Sabahno, H., Amiri, A. & Castagliola, P. 2021. A new adaptive control chart for the simultaneous monitoring of the mean and variability of multivariate normal processes. *Computers & Industrial Engineering* 151(1): 106524.

Stoumbos, Z.G. & Reynolds Jr., M.R. 1997. Control charts applying a sequential test at fixed sampling intervals. *Journal of Quality Technology* 29(1): 21-40.

Teh, S.Y., Khoo, M.B.C., Ong, K.H., Soh, K.L. & Teoh, W.L. 2015. A study on the S^2-EWMA chart for monitoring the process variance based on the MRL performance. *Sains Malaysiana* 44(7): 1067-1075.

Teoh, J.W., Teoh, W.L., Khoo, M.B.C., Celano, G. & Chong, Z.L. 2023. Optimal designs of the omnibus SPRT control chart for joint monitoring of process mean and dispersion. *International Journal of Production Research* 62(12): 4202-4225.

Zwillinger, D., & Kokoska, S. 1999. *CRC Standard Probability and Statistics Tables and Formulae.* Boca Raton: CRC Press.

*Corresponding author; email: wei_lin.teoh@hw.ac.uk